

# Supporting Information for “Evaluation of a Cyclopentane-Based $\gamma$ -Amino Acid for the Ability to Promote $\alpha/\gamma$ -Peptide Secondary Structure”

Michael W. Giuliano,\*\* Stacy J. Maynard, Aaron M. Almeida, Andrew Reidenbach, Li Guo, Emily C. Ulrich, Iliia A. Guzei, and Samuel H. Gellman\*

*Department of Chemistry, University of Wisconsin-Madison, Madison, Wisconsin 53705, United States.*

\*corresponding author: [gellman@chem.wisc.edu](mailto:gellman@chem.wisc.edu)

\*\* current address: Department of Chemistry, Yale University; [michael.giuliano@yale.edu](mailto:michael.giuliano@yale.edu)

---

<b>Table of Contents</b>	<b>Pages</b>
<b>I. Additional Synthetic Procedures</b> .....	S2-5
<b>Ia. Development of an Enantioselective Conjugate Addition</b> .....	S3-5
Reaction optimization.....	S3-4
ee determination by HPLC.....	S5
<b>II. Tabulated 2D NMR Data for <math>\alpha/\gamma</math>-peptides 9, 12, and 15</b> .....	S6-14
<b>Ila. Aggregation Control Experiment for <math>\alpha/\gamma</math>-peptide 15</b> .....	S12
<b>Ilb. DMSO Titration of <math>\alpha/\gamma</math>-peptide 15</b> .....	S13-14
<b>III. NMR Structure Calculations for <math>\alpha/\gamma</math>-peptides 9, 12, and 15</b> .....	S15-16
<b>IV. References</b> .....	S17
<b>V. 2D NMR Spectra for <math>\alpha/\gamma</math>-peptides 9, 12, and 15</b> .....	S18-28
<b>VI. 1D NMR Spectra for All New Compounds</b> .....	S29-52
<b>VII. Crystallographic Report for Dipeptide 3</b> .....	S53-64
(note: crystallographic report presented with its own references)	

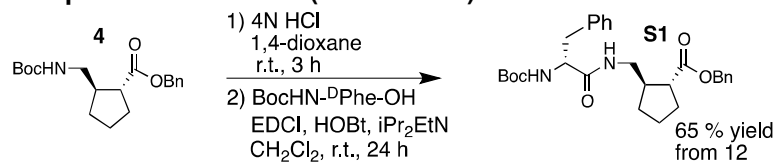
---

note: All structural figures prior to section VII of this supporting information were prepared with Pymol.<sup>1</sup> Statistics and structural ensembles for  $\alpha/\gamma$ -peptides **9**, **12**, and **15** were generated using CNS software.<sup>2</sup>

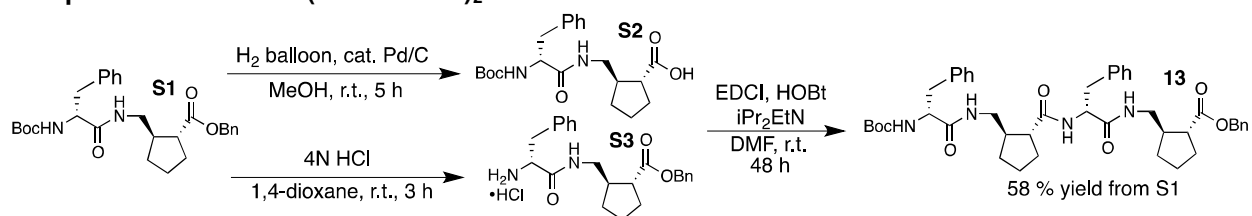
## I. Additional Synthetic Procedures

### Schemes:

#### Compound S1: Boc-HN-(<sup>D</sup>Phe-AMCP)-OBn.



#### Compound 13: Boc-HN-(<sup>D</sup>Phe-AMCP)<sub>2</sub>-OBn.



## Ia. Development of an Enantioselective Conjugate Addition.

Previously, we reported on the enantioselective conjugate addition of aldehydes to 1-nitrocyclohexene as a route to enantiopure  $\gamma$ -amino acids.<sup>3</sup> In this study, we sought  $\gamma$ -amino acids that possessed a five-membered ring across the C $\alpha$ -C $\beta$  bond. We briefly summarize our efforts in the optimization of the conjugate addition of nitromethane to 1-cyclopentene-1-carboxaldehyde.

**Reaction screening:** Reaction optimization screens were run according conjugate addition procedure detailed for the preparation of nitroalcohol **1** (crude mixtures were analyzed without the borohydride reduction step) in clean, dried 4 mL vials equipped with micro stir bars and Teflon lined caps. In cases where small (<10  $\mu$ L) volumes of reagents were required, more concentrated solutions of the reagent were prepared in the reaction solvent and added in the appropriate quantity by dilution into the reaction medium. Reactions were run on a scale of 0.5 mmol 1-cyclopentene-1-carboxaldehyde substrate at a concentration of 0.5 M (1 mL total volume).

**Determination of conversion and diastereomeric ratio by  $^1\text{H}$  NMR of crude reaction mixtures:** Reaction diastereoselectivity and conversion in the below were determined via integration of the aldehyde resonances in the  $^1\text{H}$  NMR spectra of crude reaction mixtures. A 60  $\mu$ L aliquot of reaction mixture was diluted with 600  $\mu$ L  $\text{CDCl}_3$  (w/ 0.03 % TMS) in a 5 mm NMR tube. Reliable integration of the aldehyde region required either 32 or 64 scan  $^1\text{H}$  1D data collections. A typical analysis is shown below.

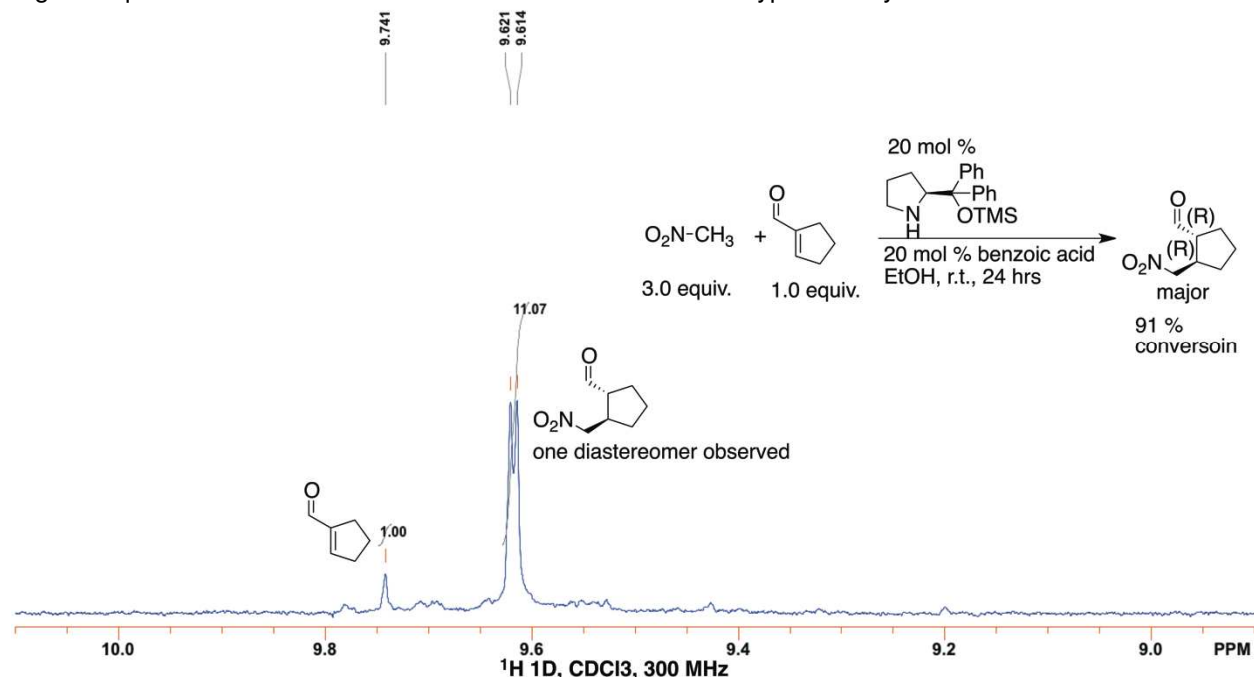
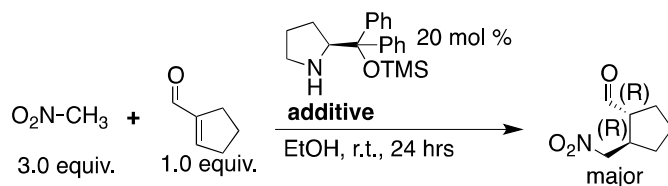


**Figure S1.** Determination of dr for nitromethane addition to 1-cyclopentene-1-carboxaldehyde from  $^1\text{H}$  NMR of crude reaction mixture (Table S1, entry 1). Structures indicate aldehyde peaks used for conversion and dr calculation. 1,2-addition products were not observed in this or any other condition. Stereochemical configuration of only observed product was assigned as (R,R) on the basis of the crystal structure of dipeptide **3**.

**Acid/Basic Additive Screening:** We screened additives for the conjugate addition of nitromethane to 1-cyclopentene-1-carboxaldehyde (Table S1). Following a brief literature survey, we proposed that a mixture of Brønsted acid<sup>4,5</sup> and amine base<sup>6,7</sup> additives may provide a synergistic effect on the conversion and/or reaction time. Following a survey of Brønsted acidic additives, from which we find benzoic acid or acetic acid as equally effective co-catalysts (entries 1 and 3), we arrived at an optimized mixture of 2,4,6-collidine and benzoic acid (entry 7). These conditions yield a single observable diastereomer in the <sup>1</sup>H NMR spectrum of the crude reaction and shorten the reaction time from 24 hours to 2 hours at room temperature.

**Table S1.** Screening of additives for the conjugate addition of nitromethane to 1-cyclopentene-1-carboxaldehyde.



entry	additive 1	additive 2	Conv. (%) <sup>a</sup>	dr (major:minor) <sup>a</sup>
1	20 mol % benzoic acid	none	91	1:0
2	20 mol % <i>m</i> -nitro benzoic acid	none	83	9:1
3	20 mol % acetic acid	none	94	1:0
4	20 mol % H <sub>2</sub> O	none	90	1:0
5	15 mol % benzoic acid	5 mol % 2,4,6-collidine	90	1:0
6	10 mol % benzoic acid	10 mol % 2,4,6-collidine	92	1:0
<b>7<sup>b</sup></b>	<b>5 mol % benzoic acid</b>	<b>15 mol % 2,4,6-collidine</b>	<b>97<sup>b</sup></b>	<b>1:0</b>

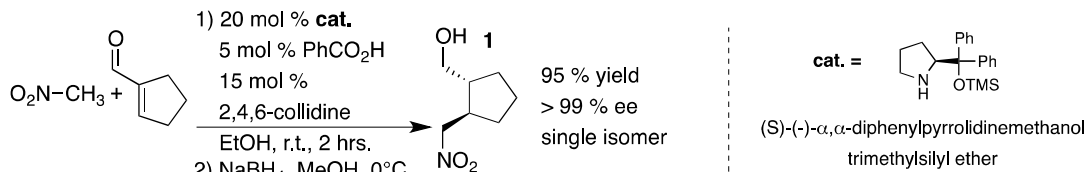
<sup>a</sup>Determined as illustrated above via analysis of the crude reaction mixture by <sup>1</sup>H NMR.

<sup>b</sup>Reaction was complete to > 90% conversion in 2 hours.

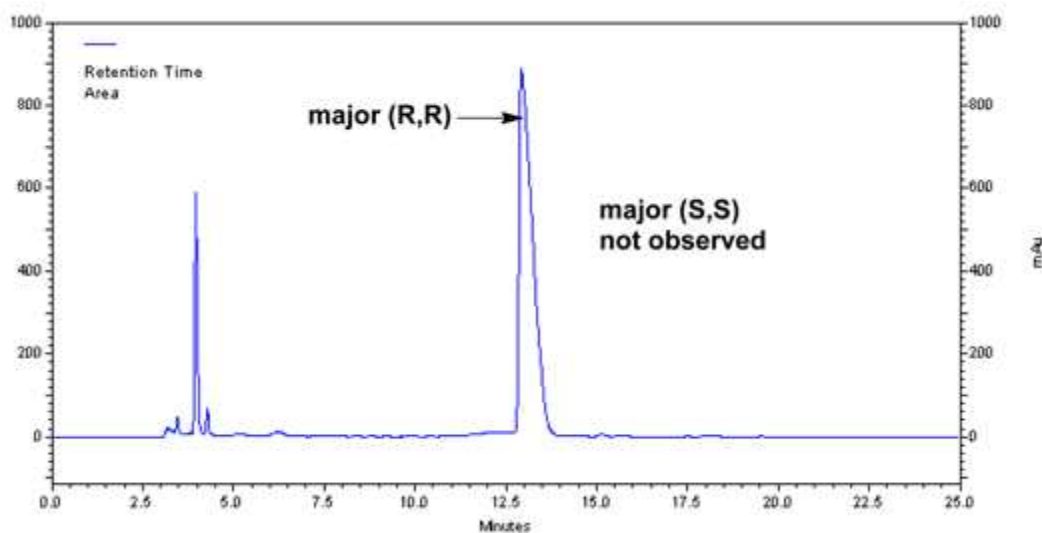
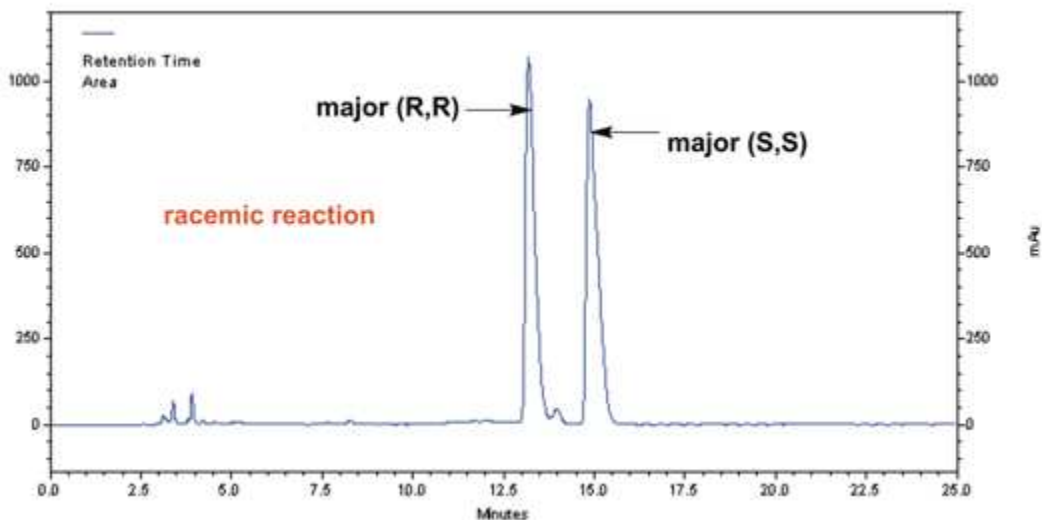


**HPLC traces for ee determination of nitroalcohol 1:** Samples were dissolved in approximately 5-10% (v/v) iPrOH in hexanes (solvents are Aldrich HPLC grade) and analyzed from 1-5  $\mu$ L injections. All columns were analytical size – 4.6 mm x 250 mm. Racemic nitroalcohol product was obtained by running conjugate addition with 10 mol % of each enantiomer of the pyrrolidine catalyst using the optimized procedure for the synthesis of nitroalcohol 1. The HPLC trace of this material is shown above that of the optimized reaction.

**optimized reaction:**

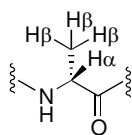
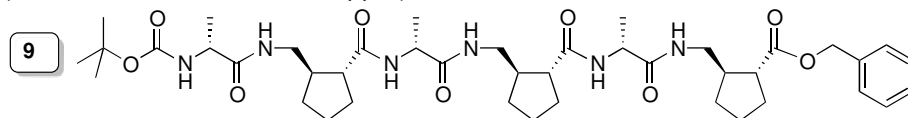


**Chromatograms:** Chiracel OJ-H column, 40°C, 1 mL/min., isocratic at 5% (v/v) iPrOH in hexanes. Retention time (R,R) configuration of major product = 13.2 min. Retention time (S,S) configuration of major product = 14.8 min. Product observed in > 99% ee for the (R,R) configuration of the major product. No integrable peak for the (S,S) configuration was observed.

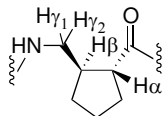


## II. Tabulated 2D NMR Data for $\alpha/\gamma$ -peptides **9**, **12**, and **15**

**Table S2.** Assigned  $^1\text{H}$  chemical shifts for  $\alpha/\gamma$ -peptide hexamer **9**  
(chemical shift error =  $\pm 0.02$  ppm)



$^{\text{D}}$ Alanine

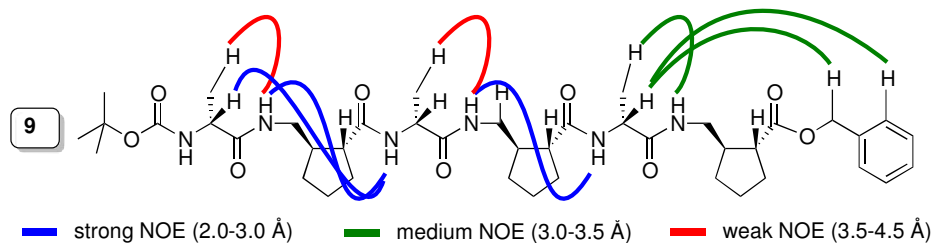


AMCP

	H $\alpha$	H $\beta$	H $\gamma_1$	H $\gamma_2$	NH	CH2	HAr
$^{\text{D}}$ Ala(1)	4.12	1.35	-	-	5.09	-	-
AMCP(2)	2.31	-	3.22	3.53	7.45	-	-
$^{\text{D}}$ Ala(3)	4.31	1.32	-	-	7.96	-	-
AMCP(4)	2.29	-	3.10	3.54	7.67	-	-
$^{\text{D}}$ Ala(5)	4.26	1.22	-	-	8.28	-	-
AMCP(6)	2.55	2.34	3.10	3.38	6.64	-	-
Benzyl	-	-	-	-	-	5.14	7.36

A note on unassigned resonances: The non-backbone ring protons of AMCP were overlapped with each other such that their chemical shifts could not be uniquely assigned. This was also the case of the  $\beta$ -protons of most AMCP residues. Unassigned crosspeaks are indicated on the 2D spectra for **9** in section V of this supporting information.

**Table S3.** Structural NOEs for  $\alpha/\gamma$ -peptide hexamer **9**  
(shown for two protons between given residues, *i* and *j*)



very strong NOE: 2.0-2.5 Å

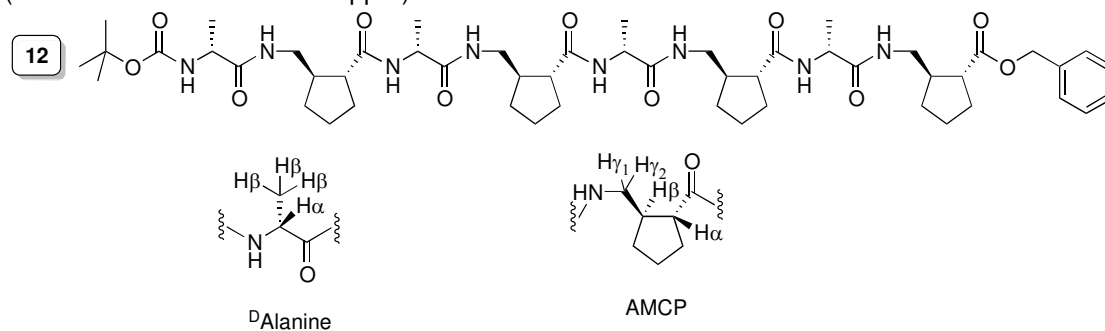
strong NOE: 2.0-3.0 Å

medium NOE: 3.0-3.5 Å

weak NOE: 3.5-4.5 Å

Residue (i)	Residue (j)	Integrated Distance (Å)	Designation
<sup>D</sup> Ala(1) H $\alpha$	<sup>D</sup> Ala(3) NH	2.9	strong
<sup>D</sup> Ala(1) H $\beta$	AMCP(2) NH	4.3	weak
AMCP(2) NH	<sup>D</sup> Ala(3) NH	2.9	strong
<sup>D</sup> Ala(3) H $\beta$	AMCP(4) NH	4.5	weak
AMCP(4) NH	<sup>D</sup> Ala(5) NH	2.9	strong
<sup>D</sup> Ala(5) H $\alpha$	Benzyl HAr	3.2	medium
<sup>D</sup> Ala(5) H $\alpha$	Benzyl CH <sub>2</sub>	3.2	medium
<sup>D</sup> Ala(5) H $\beta$	AMCP(6) NH	3.6	weak

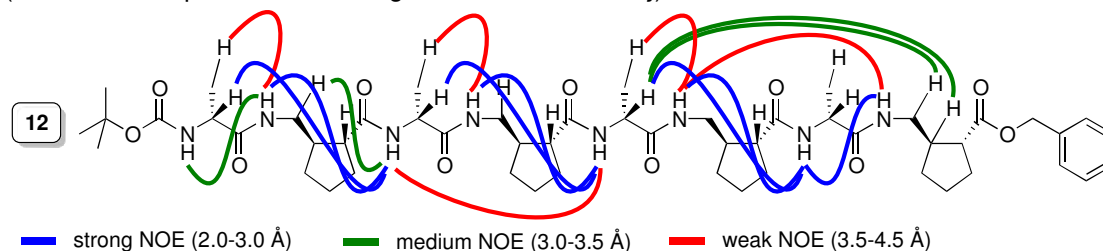
**Table S4.** Assigned  $^1\text{H}$  chemical shifts for  $\alpha/\gamma$ -peptide octamer **12**  
(chemical shift error =  $\pm 0.02$  ppm)



	$\text{H}\alpha$	$\text{H}\beta$	$\text{H}\gamma_1$	$\text{H}\gamma_2$	$\text{NH}$	$\text{CH}_2$	$\text{HAr}$
$^{\text{D}}\text{Ala}(1)$	4.20	1.36	-	-	5.11	-	-
$\text{AMCP}(2)$	2.33	-	3.20	3.54	7.47	-	-
$^{\text{D}}\text{Ala}(3)$	4.42	1.36	-	-	7.95	-	-
$\text{AMCP}(4)$	2.33	-	3.12	3.58	7.71	-	-
$^{\text{D}}\text{Ala}(5)$	4.30	1.27	-	-	8.72	-	-
$\text{AMCP}(6)$	2.31	-	3.07	3.55	7.76	-	-
$^{\text{D}}\text{Ala}(7)$	4.26	1.22	-	-	8.36	-	-
$\text{AMCP}(8)$	2.35	2.54	3.09	3.44	6.61	-	-
Benzyl	-	-	-	-	-	5.14	7.36

**A note on unassigned resonances:** The non-backbone ring protons of AMCP were overlapped with each other such that their chemical shifts could not be uniquely assigned. This was also the case of the  $\beta$ -protons of most AMCP residues. Unassigned crosspeaks are indicated on the 2D spectra for **12** in section V of this supporting information.

**Table S5.** Structural NOEs for  $\alpha/\gamma$ -peptide octamer **12**  
(shown for two protons between given residues, *i* and *j*)



very strong NOE: 2.0-2.5 Å

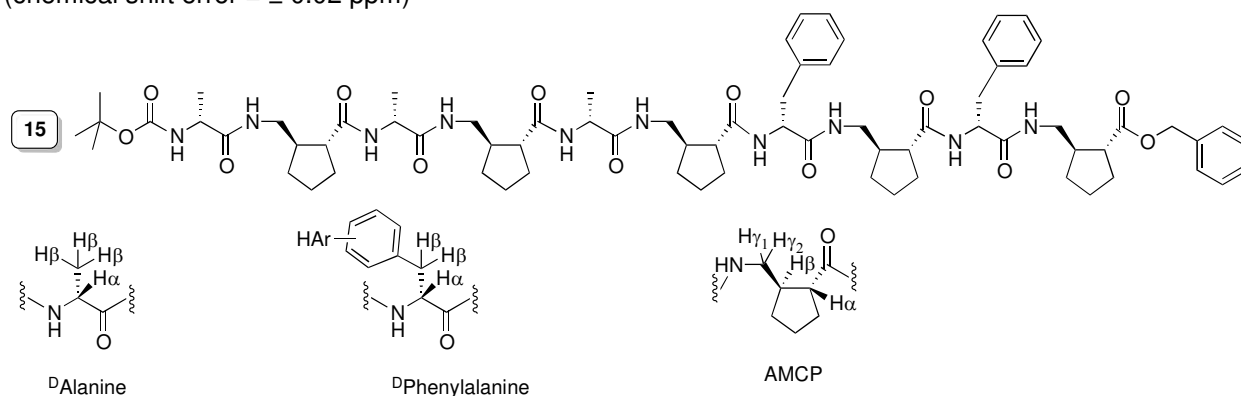
strong NOE: 2.5-3.0 Å

medium NOE: 3.0-3.5 Å

weak NOE: 3.5-4.5 Å

Residue (i)	Residue (j)	Integrated Distance (Å)	Designation
<sup>D</sup> Ala(1) H $\alpha$	<sup>D</sup> Ala(3) NH	2.6	strong
<sup>D</sup> Ala(1) H $\beta$	AMCP(2) NH	4.1	weak
<sup>D</sup> Ala(1) NH	AMCP(2) NH	3.4	medium
AMCP(2) NH	<sup>D</sup> Ala(3) NH	2.5	strong
AMCP(2) H $\gamma$	<sup>D</sup> Ala(3) NH	3.2	medium
<sup>D</sup> Ala(3) H $\alpha$	<sup>D</sup> Ala(5) NH	2.4	very strong
<sup>D</sup> Ala(3) H $\beta$	AMCP(4) NH	4.3	weak
<sup>D</sup> Ala(3) NH	<sup>D</sup> Ala(5) NH	3.9	weak
AMCP(4) NH	<sup>D</sup> Ala(5) NH	2.4	very strong
<sup>D</sup> Ala(5) H $\alpha$	<sup>D</sup> Ala(7) NH	2.1	very strong
<sup>D</sup> Ala(5) H $\alpha$	AMCP(8) H $\gamma$	3.0	medium
<sup>D</sup> Ala(5) H $\alpha$	AMCP(8) H $\beta$	3.1	medium
<sup>D</sup> Ala(5) H $\beta$	AMCP(6) NH	3.5	weak
AMCP(6) NH	<sup>D</sup> Ala(7) NH	2.4	very strong
AMCP(6) NH	AMCP(8) NH	3.6	weak
<sup>D</sup> Ala(7) NH	AMCP(8) NH	2.8	strong

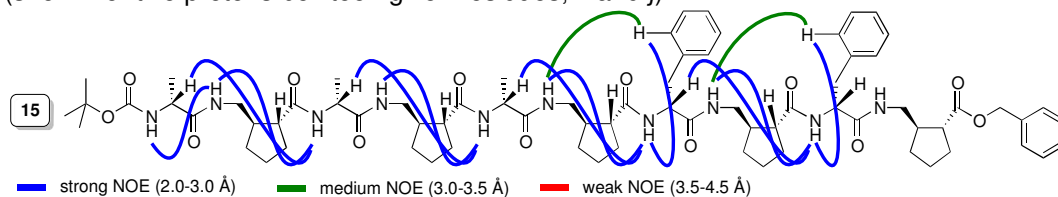
**Table S6.** Assigned  $^1\text{H}$  chemical shifts for  $\alpha/\gamma$ -peptide decamer **15**  
(chemical shift error =  $\pm 0.02$  ppm)



	H $\alpha$	H $\beta^*$	H $\gamma_1$	H $\gamma_2$	NH	CH2	HAr
$^{\text{D}}$ Ala(1)	4.18	1.35	-	-	5.59	-	-
AMCP(2)	2.31	-	3.19	3.44	7.84	-	-
$^{\text{D}}$ Ala(3)	4.33	1.38	-	-	7.98	-	-
AMCP(4)	2.37	-	3.12	3.51	8.10	-	-
$^{\text{D}}$ Ala (5)	4.45	1.33	-	-	8.59	-	-
AMCP (6)	2.34	-	3.10	3.48	8.08	-	-
$^{\text{D}}$ Phe (7)	4.60	2.97	-	-	8.48	-	7.35
AMCP (8)	2.18	-	2.98	3.40	7.74	-	-
$^{\text{D}}$ Phe (9)	4.46	2.92	-	-	8.14	-	7.19
AMCP (10)	2.23	-	3.10	3.23	6.96	-	-
Benzyl	-	-	-	-	-	5.09	7.33

**A note on unassigned resonances:** The non-backbone ring protons of AMCP were overlapped with each other such that their chemical shifts could not be uniquely assigned. This was also the case of the  $\beta$ -protons of AMCP residues. Unassigned crosspeaks are indicated on the 2D spectra for **15** in section V of this supporting information. \* Diastereotopic  $\beta$ -protons of  $^{\text{D}}$ Phe residues were not resolved, thus a single chemical shift for each methylene unit is reported.

**Table S7.** Structural NOEs for  $\alpha/\gamma$ -peptide decamer **15**  
(shown for two protons between given residues, *i* and *j*)



very strong NOE: 2.0-2.5 Å

strong NOE: 2.5-3.0 Å

medium NOE: 3.0-3.5 Å

weak NOE: 3.5-4.5 Å

Residue (i)	Residue (j)	Integrated Distance (Å)	Designation
<sup>D</sup> Ala(1) H $\alpha$	<sup>D</sup> Ala(3) NH	2.4	very strong
<sup>D</sup> Ala(1) NH	AMCP(2) NH	2.6	strong
AMCP(2) NH	<sup>D</sup> Ala(3) NH	2.8	strong
<sup>D</sup> Ala(3) H $\alpha$	<sup>D</sup> Ala(5) NH	2.2	very strong
AMCP(4) NH	<sup>D</sup> Ala(5) NH	2.2	very strong
<sup>D</sup> Ala(5) H $\alpha$	<sup>D</sup> Phe(7) NH	2.2	very strong
AMCP(6) NH	<sup>D</sup> Phe(7) NH	2.1	very strong
<sup>D</sup> Phe(7) H $\alpha$	<sup>D</sup> Phe(9) NH	2.4	very strong
AMCP(8) NH	<sup>D</sup> Phe(9) NH	2.4	very strong
<sup>D</sup> Phe(9) NH	AMCP(10) NH	2.9	strong
<sup>D</sup> Phe(7) NH	<sup>D</sup> Phe(7) HAr	2.9	strong
AMCP(6) NH	<sup>D</sup> Phe(7) HAr	3.2	medium
<sup>D</sup> Phe(9) NH	<sup>D</sup> Phe(9) HAr	3.4	medium

## Ila. Aggregation Control Experiment for $\alpha/\gamma$ -peptide **15**

The solubility of  $\alpha/\gamma$ -peptides composed of hydrophobic residues tends to decrease with peptide length. Therefore, if we conclude that **15** is not aggregated in solution, we suspect that **9** and **12** which show very similar spectral characteristics to **15** (albeit in  $\text{CDCl}_3$  solution; dissolution of **15** required 5 %  $\text{CD}_3\text{OH}$  by volume to prevent gelation of the sample), are also not aggregated in solution. We subjected  $\alpha/\gamma$ -peptide decamer **15** to a dilution experiment, in which  $^1\text{H}$  1D spectra were taken at each concentration. If **15** aggregates in solution under the conditions of our experiments, then we would expect that as concentration decreases, the dispersion of proton resonances in the  $^1\text{H}$  1D spectrum of **15** would decrease as the local environment around each proton becomes less anisotropic due to the break up and dissolution of aggregates at lower concentrations. However, if **15** is not aggregated, we would expect there to be little to no change in the chemical shifts of the proton resonances in the  $^1\text{H}$  1D NMR spectrum across all measured concentrations. We feel that decamer **15** is representative of the peptides in the present work as it is the longest of the sequence and exhibited the lowest solubility. This study is summarized below.

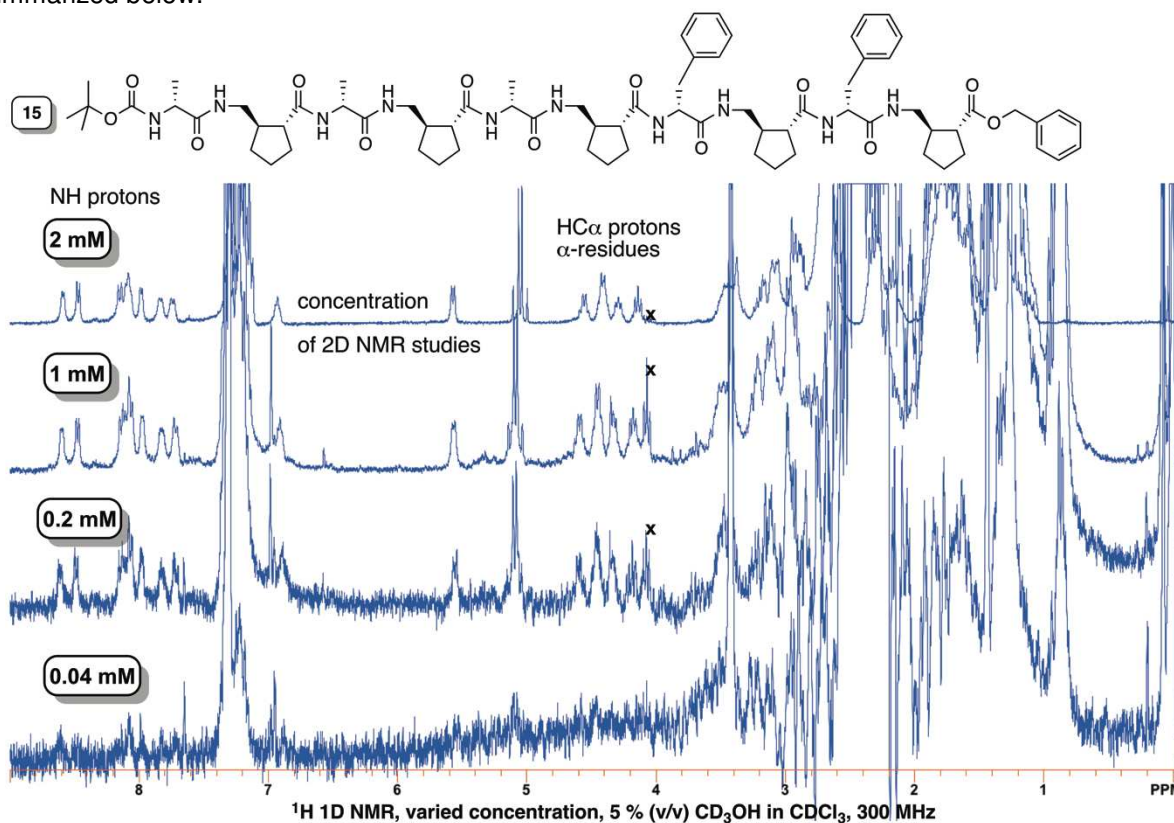


**Figure S2.** Variable concentration  $^1\text{H}$  1D NMR spectra of  $\alpha/\gamma$ -peptide decamer **15** in 5 %  $\text{CD}_3\text{OH}$  in  $\text{CDCl}_3$  (0.03 % TMS). The concentration of each trace is indicated above.

We *do not* observe changes in the chemical shifts of the NH proton or  $\alpha$ -residue HC $\alpha$  proton resonances of  $\alpha/\gamma$ -peptide decamer **15** over a 50-fold range of concentration; overlap of other resonances with each other and the solvent peak of  $\text{CD}_3\text{OH}$  precluded meaningful observation in this experiment. We are therefore confident that **15** is not aggregated in our NMR studies. All three samples remained in solution (**9** and **12** in neat  $\text{CDCl}_3$ ; **15** with the addition of 5 %  $\text{CD}_3\text{OH}$  co-solvent) for more than one week without observation of gelation or precipitation. The latter only occurred for **15**, and only after  $\text{CDCl}_3$  had evaporated from the co-solvent mixture over the course of more than two weeks. We therefore believe that the NMR observations reported for these  $\alpha/\gamma$ -peptides arise from the folding preferences of individual peptide molecules and not from the influence of some type of aggregation induced conformation.



## IIb. DMSO titration of NMR sample of $\alpha/\gamma$ -peptide **15**

In an effort to gain more information about the nature of the structure of AMCP-containing  $\alpha/\gamma$ -peptides **9**, **12**, and **15** that leads to the observed repeated NOE pattern, we subjected the NMR sample of decamer **15**, for which we observe the longest chain of this pattern, to a  $d_6$ -DMSO titration. Protons that are exposed to solvent will interact with the oxygen of  $d_6$ -DMSO solvent molecules and exhibit downfield shifting of their resonances with increasing volumes of added  $d_6$ -DMSO. By contrast, protons that are not exposed to solvent due to intramolecular hydrogen bonding will shift to a much lesser degree, often in the upfield direction. The data for  $\alpha/\gamma$ -peptide **15** is depicted in a bar graph and discussed in detail in the manuscript. Below we present the stack plot of the NH proton region of the 1D  $^1\text{H}$  NMR spectrum of **15** with volume of added DMSO indicated for each trace. Tables of the measured chemical shifts and calculated chemical shift changes for each proton at each concentration (used to generate the graph in the manuscript) are also included.

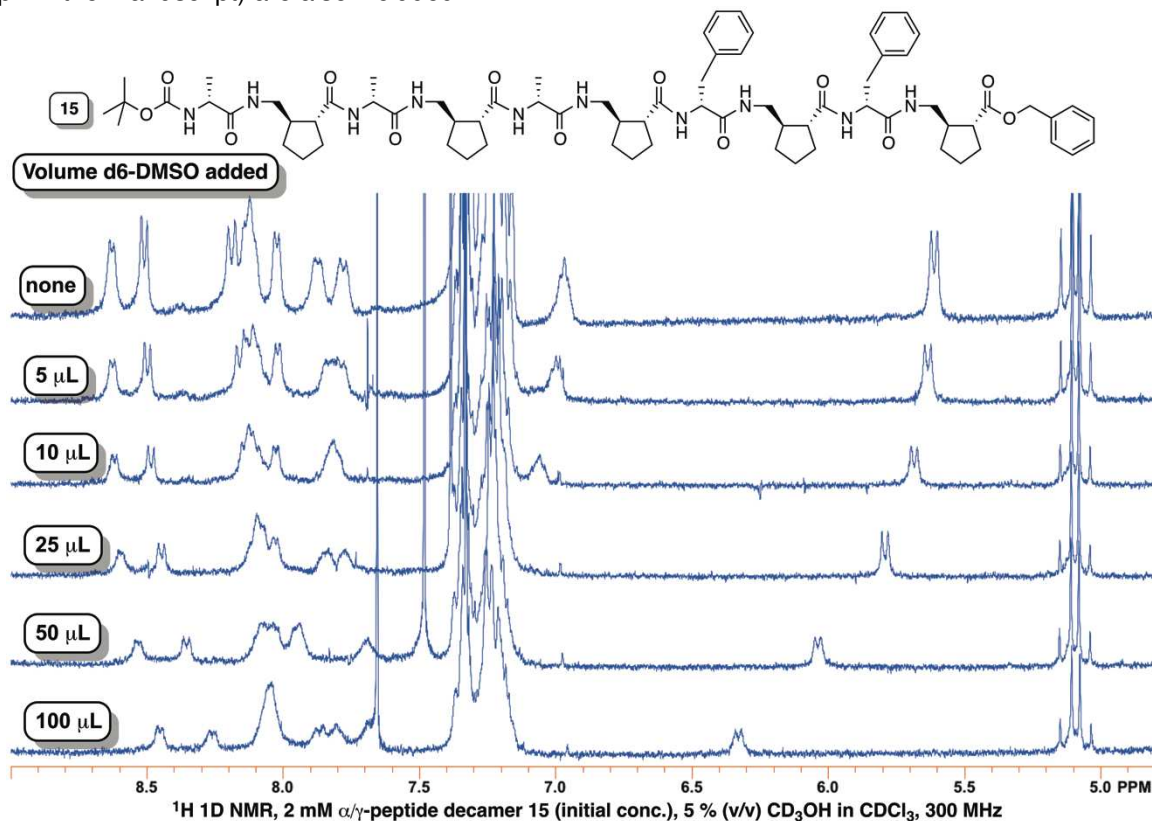


**Figure S3.** Stacked amide regions of 1D  $^1\text{H}$  NMR spectra of titrated  $\alpha/\gamma$ -peptide decamer **15** (300 MHz,  $\text{CDCl}_3$  with 5% (v/v)  $\text{CD}_3\text{OH}$ ) Volume of added  $d_6$ -DMSO is indicated with each trace.

**Table S8.** Measured Chemical shifts of amide NH protons of  $\alpha/\gamma$ -peptide decamer **15** during DMSO titration experiment.

Vol. $d_6$ -DMSO ( $\mu$ L)	0	5	10	25	50	100
Amide NH	$\delta$ (ppm)	$\delta$ (ppm)	$\delta$ (ppm)	$\delta$ (ppm)	$\delta$ (ppm)	$\delta$ (ppm)
<sup>D</sup> Ala(1)	5.59	5.64	5.68	5.78	6.04	6.32
AMCP(2)	7.87	7.84	7.82	7.77	7.69	-
<sup>D</sup> Ala(3)	8.02	8.02	8.02	8.03	7.94	7.86
AMCP(4)	8.14	8.11	-	-	-	-
<sup>D</sup> Ala(5)	8.64	8.63	8.62	8.59	8.53	8.45
AMCP(6)	8.11	8.11	-	-	-	-
<sup>D</sup> Phe(7)	8.52	8.50	8.48	8.44	8.35	8.25
AMCP(8)	7.77	7.79	7.82	7.84	7.94	8.04
<sup>D</sup> Phe(9)	8.19	8.16	8.14	8.09	-	-
AMCP(10)	6.95	6.99	7.06	-	7.49	7.66

note: dashed entries indicate resonances that were overlapped and thus unable to be assigned unambiguously.

**Table S9.** Calculated chemical shift changes relative to zero DMSO added of amide NH protons of  $\alpha/\gamma$ -peptide decamer **15** during DMSO titration experiment.

Vol. $d_6$ -DMSO ( $\mu$ L)	5	10	25	50	100
Amide NH	$\Delta\delta$ (ppm)	$\Delta\delta$ (ppm)	$\Delta\delta$ (ppm)	$\Delta\delta$ (ppm)	$\Delta\delta$ (ppm)
<sup>D</sup> Ala(1)	0.05	0.09	0.19	0.45	0.73
AMCP(2)	-0.03	-0.05	-0.10	-0.18	-
<sup>D</sup> Ala(3)	0.00	0.00	0.01	-0.08	-0.16
AMCP(4)	-0.03	-	-	-	-
<sup>D</sup> Ala(5)	-0.01	-0.02	-0.05	-0.11	-0.19
AMCP(6)	0.00	-	-	-	-
<sup>D</sup> Phe(7)	-0.02	-0.04	-0.08	-0.17	-0.27
AMCP(8)	0.02	0.05	0.07	0.17	0.27
<sup>D</sup> Phe(9)	-0.03	0.05	-0.10	-	-
AMCP(10)	0.04	0.11	-	0.54	0.71

note: dashed entries indicate resonances that were overlapped and thus unable to be assigned unambiguously.

### III. NMR Structure Statistics and Ensembles for $\alpha/\gamma$ -peptides 9, 12, and 15

**Table S10.** Structure statistics for  $\alpha/\gamma$ -peptides 9, 12, and 15.

<b>NMR constraints</b>	<b>9</b>	<b>12</b>	<b>15</b>
<b>Distance constraints</b>			
Total NOE	9	16	13
Intra-residue	0	0	0
Inter-residue	9	16	13
Sequential ( $ i - j  = 1$ ) (not across $\gamma$ -residue)	0	0	0
Medium-range ( $ i - j  < 4$ ) (includes NOEs across $\gamma$ -residues to nearest neighbor)	9	16	13
Long-range ( $ i - j  > 5$ )	0	0	0
Intermolecular	0	0	0
Hydrogen bonds	0	0	0
<b>Total dihedral angle restraints</b>			
$\phi$	0	0	0
$\psi$	0	0	0
<b>Structure statistics</b>			
Violations (mean and s.d.)	1.00 $\pm$ 0.0**	0	0
Distance constraints ( $\text{\AA}$ )	0.01 $\pm$ 0.001	0.02 $\pm$ 0.01	0.02 $\pm$ 0.01
Dihedral angle constraints ( $^\circ$ )	0	0	0
Max. dihedral angle violation ( $^\circ$ )	55.6**	0	0
Max. distance constraint violation ( $\text{\AA}$ )	0	0	0
<b>Deviations from idealized geometry</b>			
Bond lengths ( $\text{\AA}$ )	$\pm$ 0.0047	$\pm$ 0.0047	$\pm$ 0.0052
Bond angles ( $^\circ$ )	$\pm$ 0.77	$\pm$ 0.78	$\pm$ 0.63
Impropers ( $^\circ$ )	$\pm$ 0.62	$\pm$ 0.66	$\pm$ 0.70
<b>Average pairwise r.m.s. deviation (<math>\text{\AA}</math>)</b> (10 Structures)			
Heavy	1.2 $\pm$ 0.2	3.0 $\pm$ 1.1	3.6 $\pm$ 1.0
Backbone	0.8 $\pm$ 0.1	2.0 $\pm$ 1.0	2.4 $\pm$ 0.4

\*\* We occasionally observe violation of the cyclopentyl ring dihedral restraints we manually put into CNS.

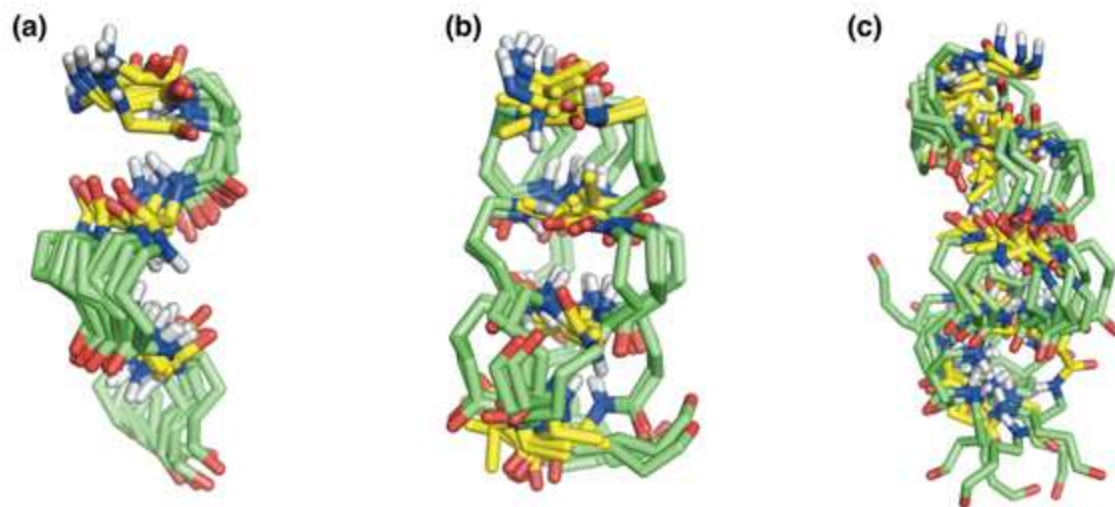


**Figure S4.** (a) Ten lowest-energy structures of  $\alpha/\gamma$ -peptide hexamer **9**. (b) Ten lowest-energy structures of  $\alpha/\gamma$ -peptide octamer **12**. (c) Ten lowest-energy structure of  $\alpha/\gamma$ -peptide decamer **15**. AMCP residues are shown in green,  $\alpha$ -residues and protecting groups are shown in yellow.

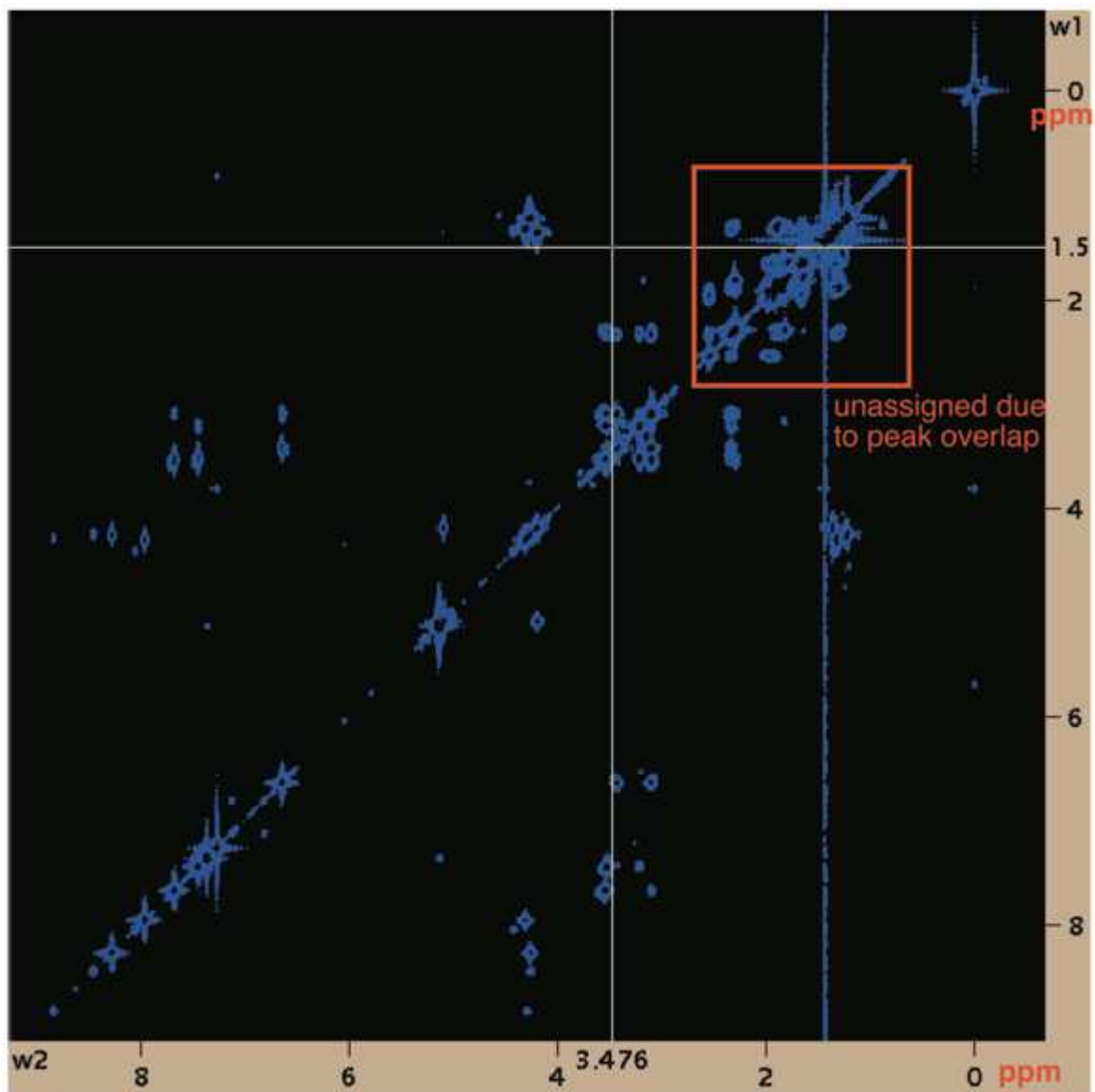
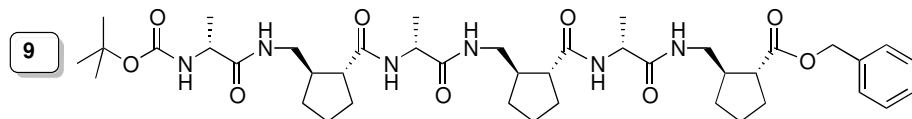
## IV. References

- 1) The PyMOL Molecular Graphics System, Version 1.5.0.4 Schrödinger, LLC.
- 2) (a) Brunger, A. T.; Adams, P. D.; Clore, G. M.; DeLano, W. L.; Gros, P.; Grosse-Kunstleve, R. W.; Jiang, J. S.; Kuszewski, J.; Nilges, M.; Pannu, N. S.; Read, R. J.; Rice, L. M.; Simonson, T.; Warren, G. L. *Acta Crystallogr., Sect. D: Biol. Crystallogr.* **1998**, *54*, 905. (b) Brunger, A. T. *Nat. Protoc.* **2007**, *2*, 2728.
- 3) Guo, L.; Chi, Y. G.; Almeida, A. M.; Guzei, I. A.; Parker, B. K.; Gellman, S. H. *J. Am. Chem. Soc.* **2009**, *131*, 16018.
- 4) Zu, L.; Xie, H.; Li, H.; Wang, H.; Wang, W. *Adv. Synth. Catal.* **2007**, *349*, 2660.
- 5) Palomo, C.; Landa, A.; Mielgo, A.; Oiarbide, M.; Puente, A.; Vera, S. *Angew. Chem. Int. Ed.* **2007**, *46*, 8431.
- 6) Hanessian, S.; Pham, V. *Org. Lett.* **2000**, *2*, 2975.
- 7) Hanessian, S.; Shao, Z. H.; Warriar, J. S. *Org. Lett.* **2006**, *8*, 4787.
- 8) Goddard, D. T.; Kneller, D. G. SPARKY 3, University of California, San Francisco.

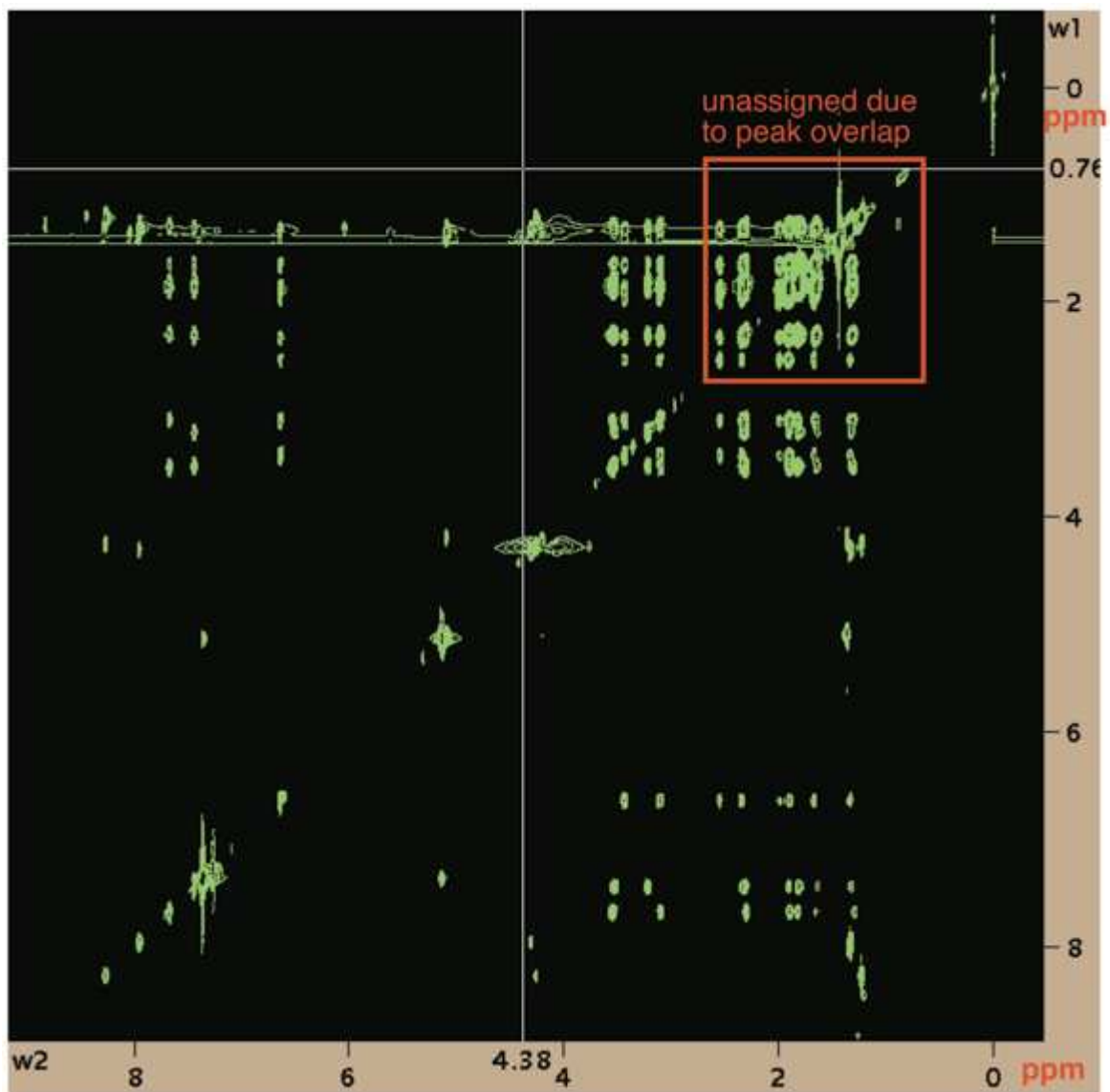
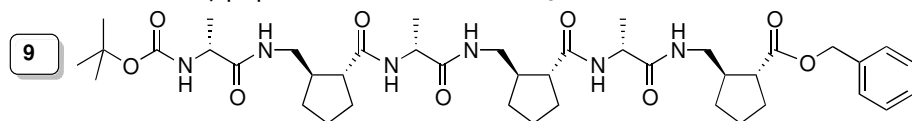
## V. 2D NMR Spectra for $\alpha/\gamma$ -peptides 9, 12 and 15

Spectra plots were generated in SPARKY,<sup>8</sup> which was used for assignment and integration of all data.

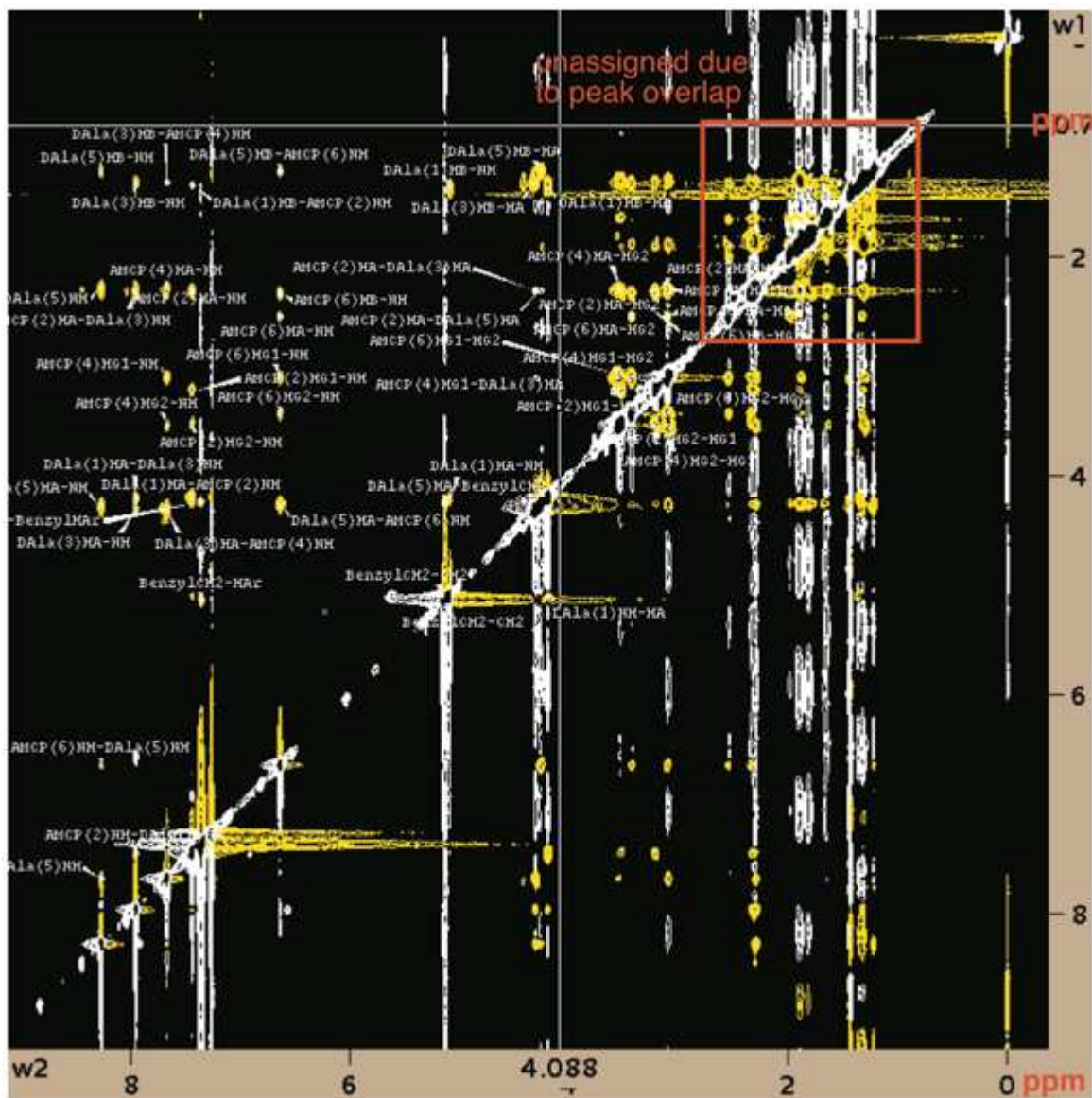
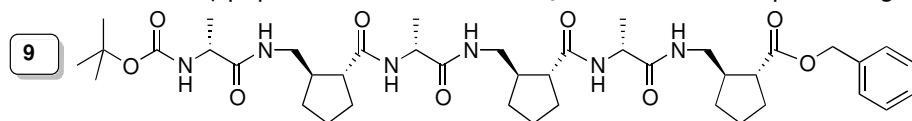
**gCOSY:** 2 mM  $\alpha/\gamma$ -peptide hexamer **9** in CDCl<sub>3</sub> solution.



**TOCSY:** 2 mM  $\alpha/\gamma$ -peptide hexamer **9** in  $\text{CDCl}_3$  solution.

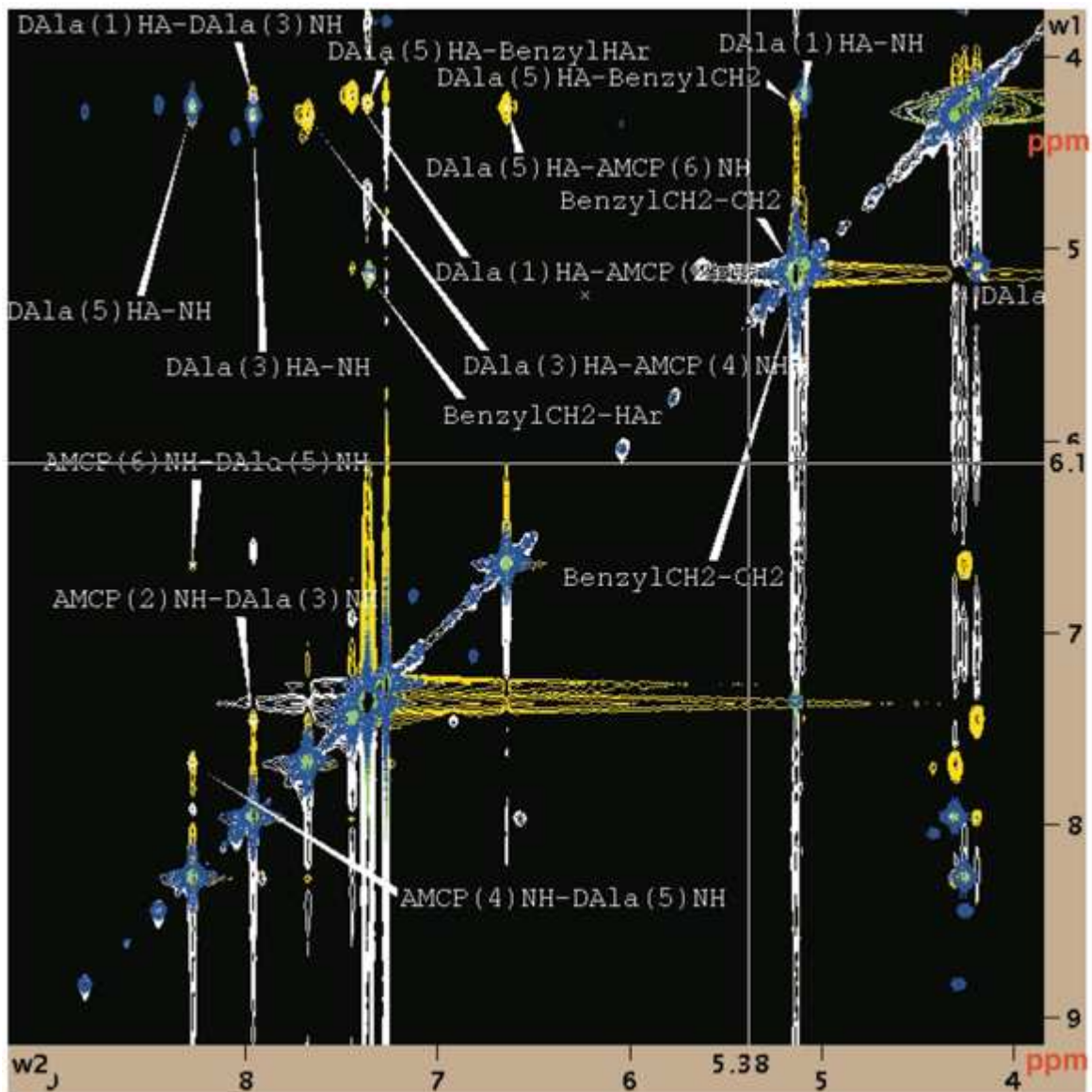
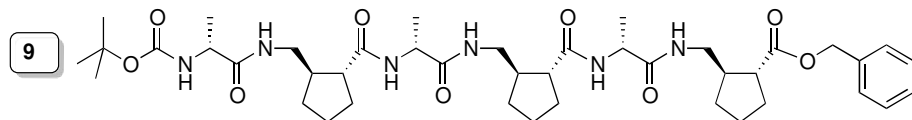


ROESY: 2 mM  $\alpha/\gamma$ -peptide hexamer **9** in  $\text{CDCl}_3$  solution. Positive peaks in gold, negative peaks in white.

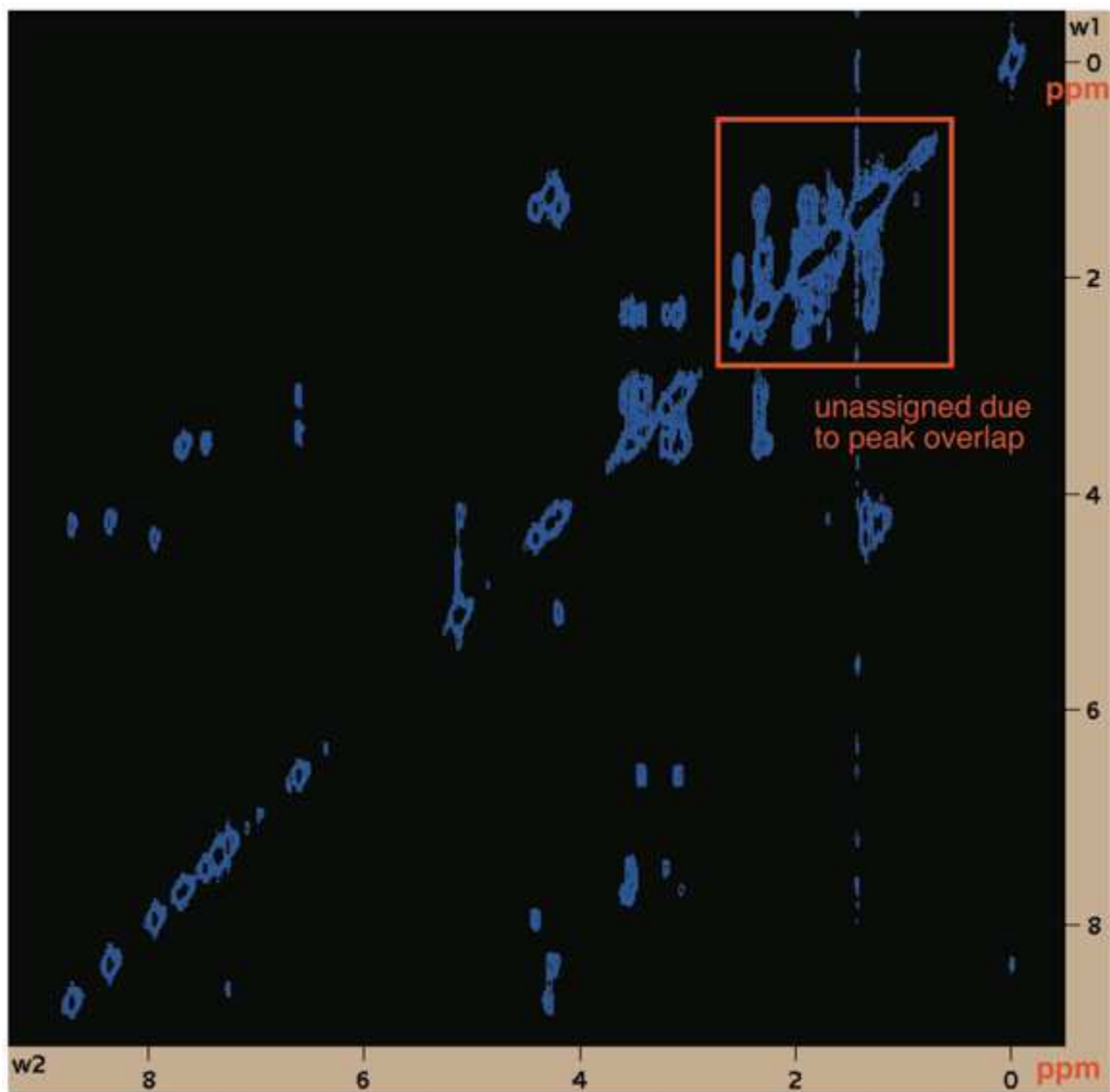
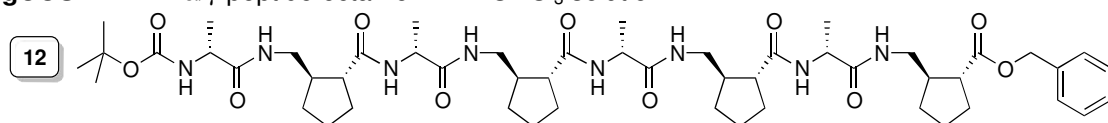




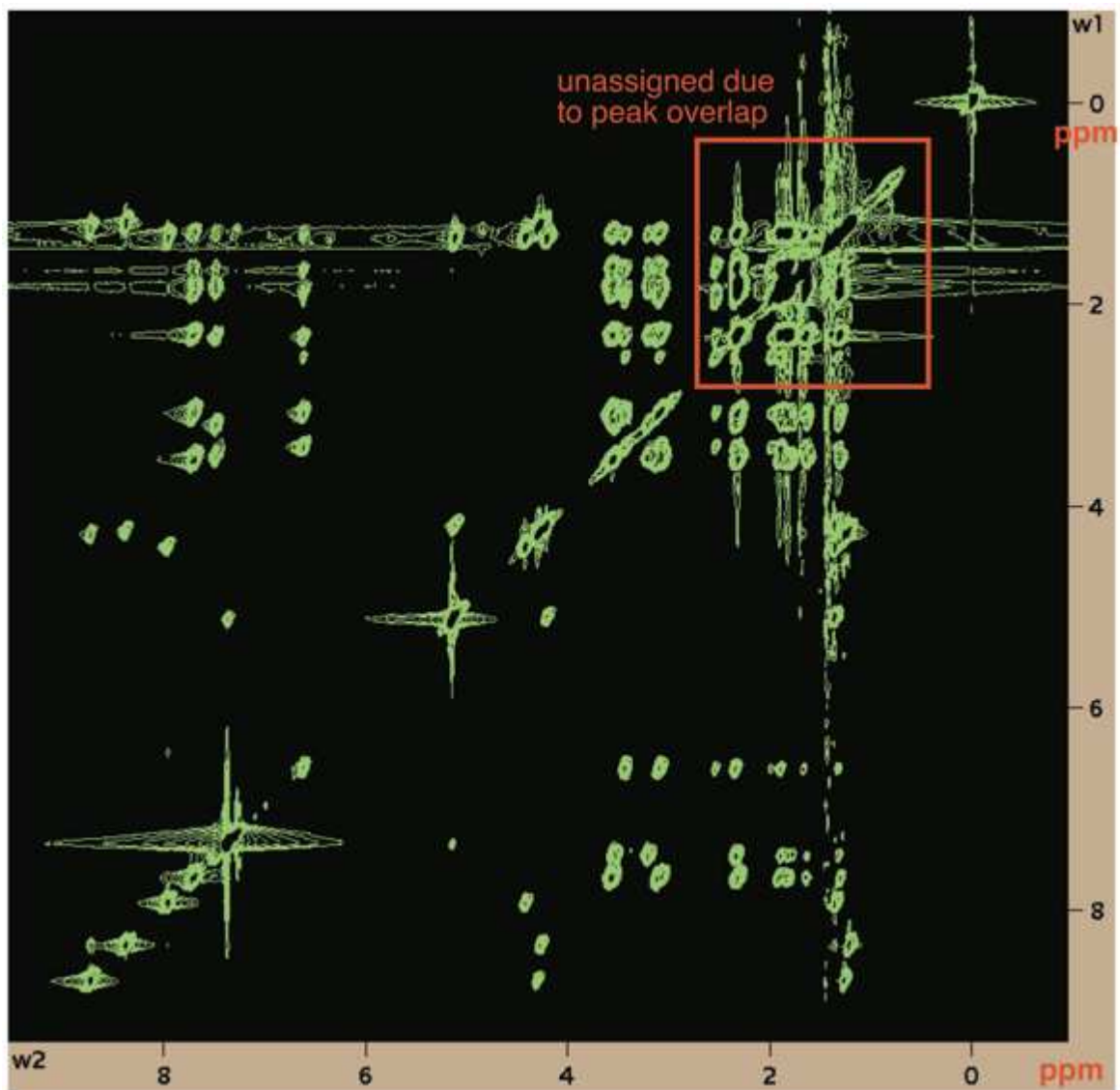
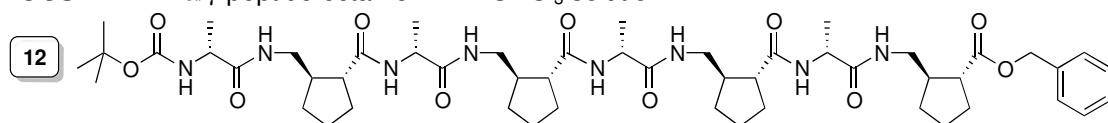
**Partial overlay of gCOSY, TOCSY, ROESY used for assignment:** 2 mM  $\alpha/\gamma$ -peptide hexamer **9** in CDCl<sub>3</sub> solution. Positive ROESY peaks in gold, negative ROESY peaks in white. TOCSY peaks are in green. gCOSY peaks are in blue.



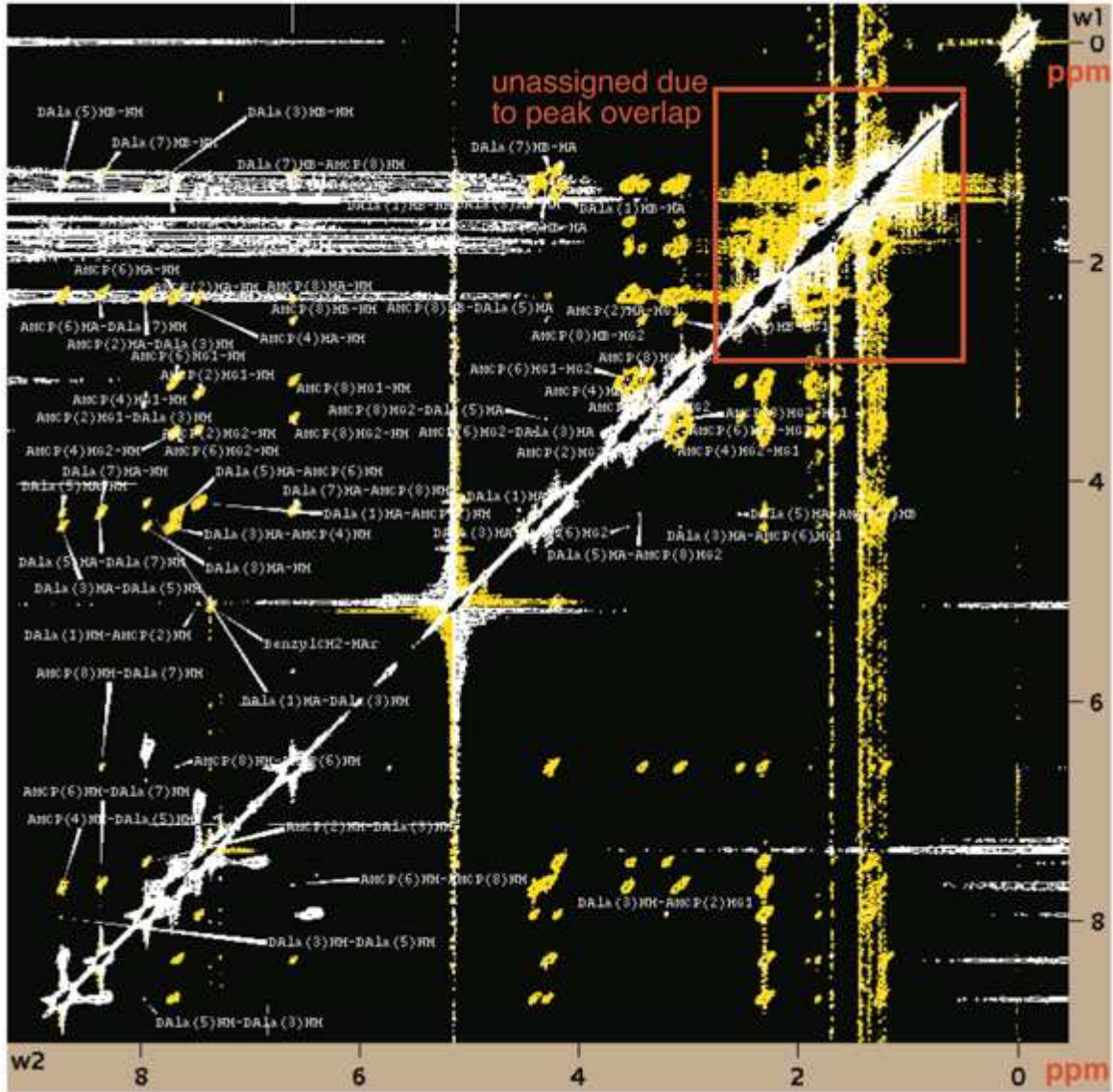
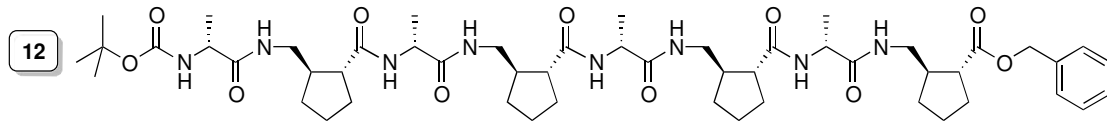
**gCOSY:** 2 mM  $\alpha/\gamma$ -peptide octamer **12** in  $\text{CDCl}_3$  solution.



**TOCSY:** 2 mM  $\alpha/\gamma$ -peptide octamer **12** in  $\text{CDCl}_3$  solution.

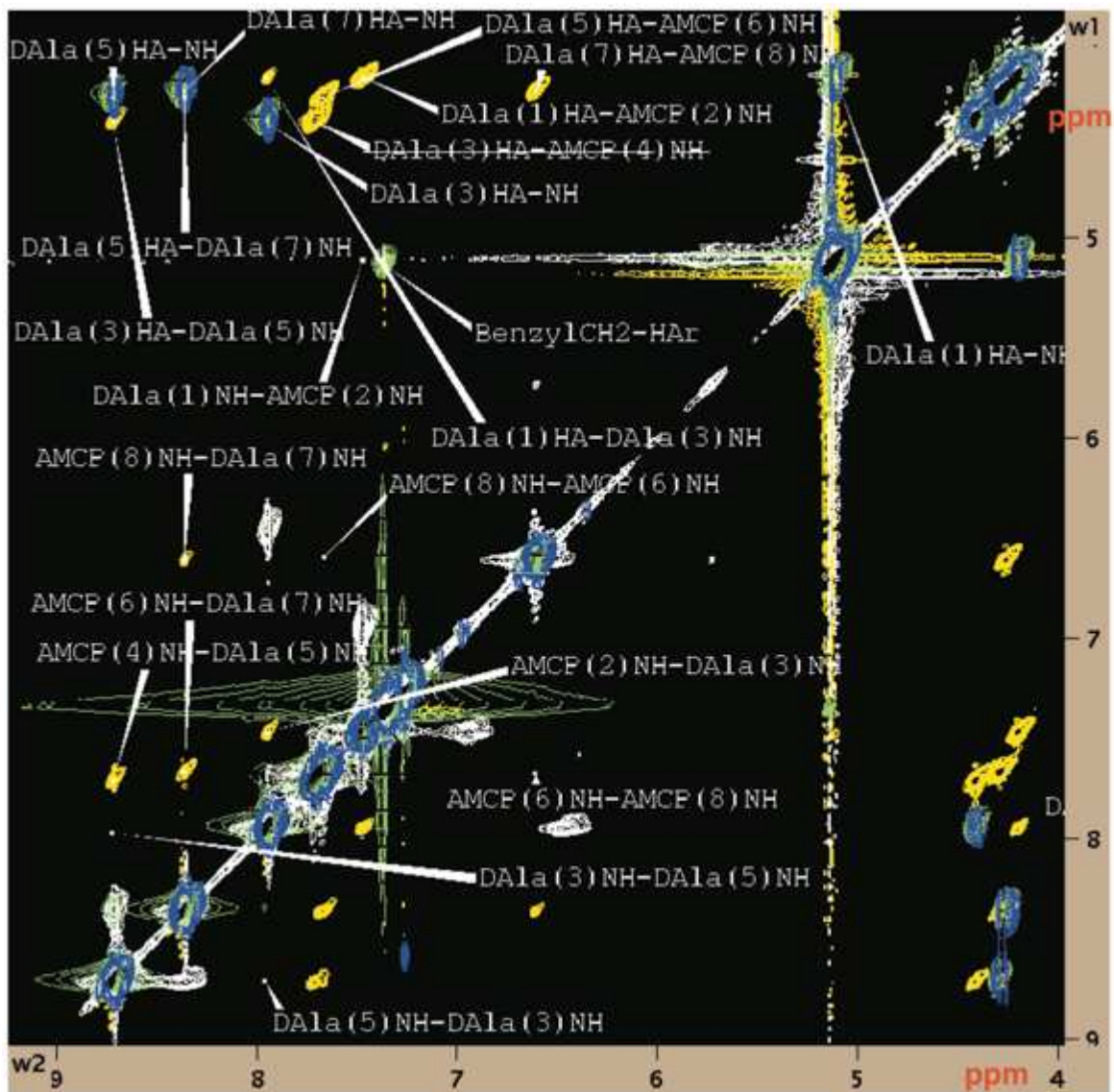
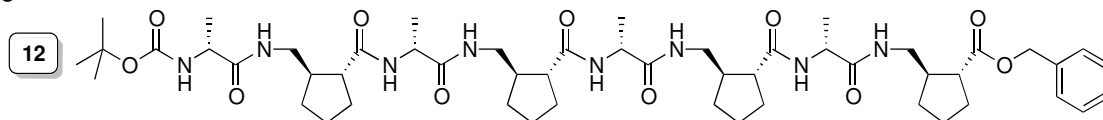


ROESY: 2 mM  $\alpha/\gamma$ -peptide octamer **12** in CDCl<sub>3</sub> solution.

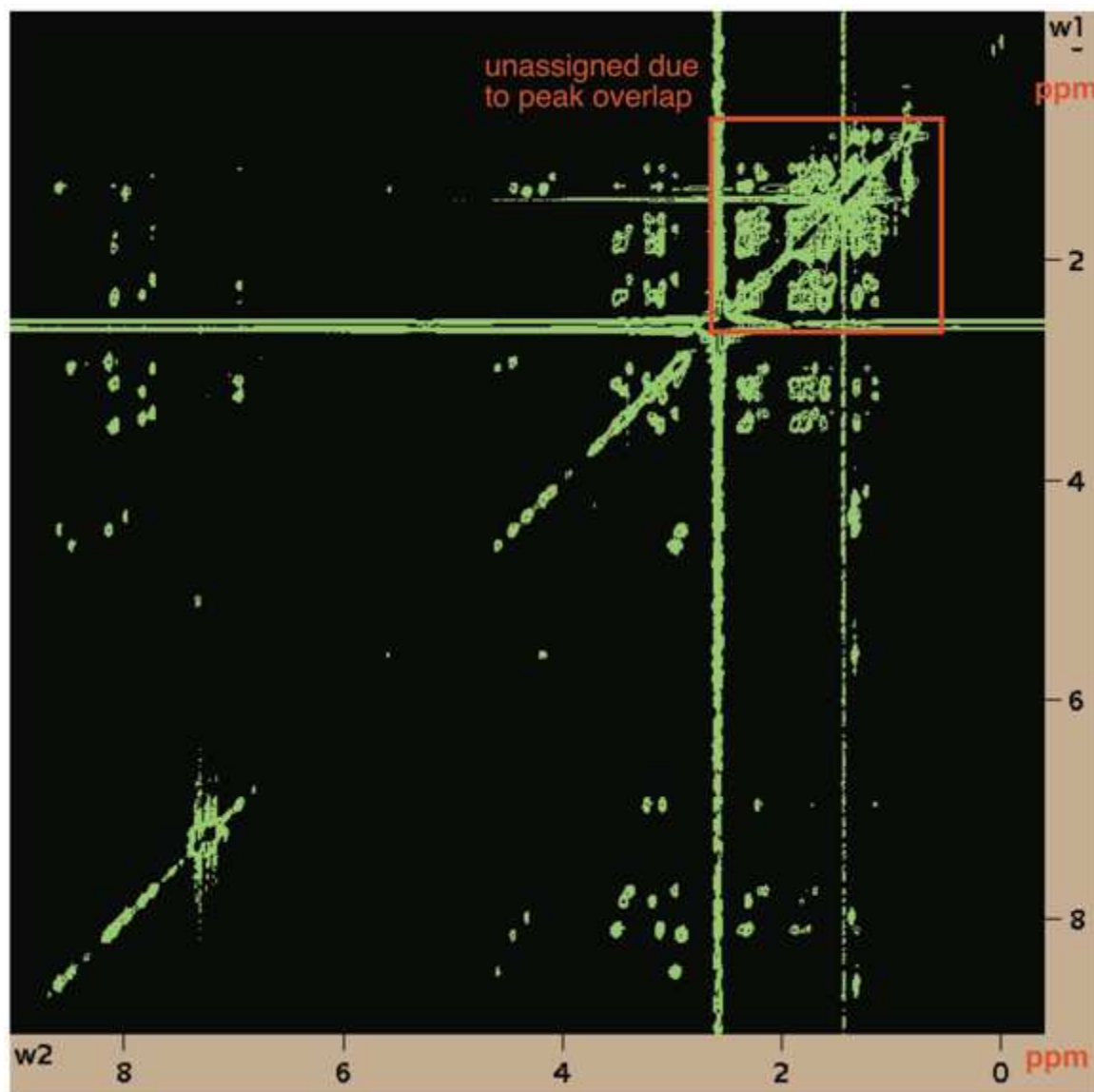
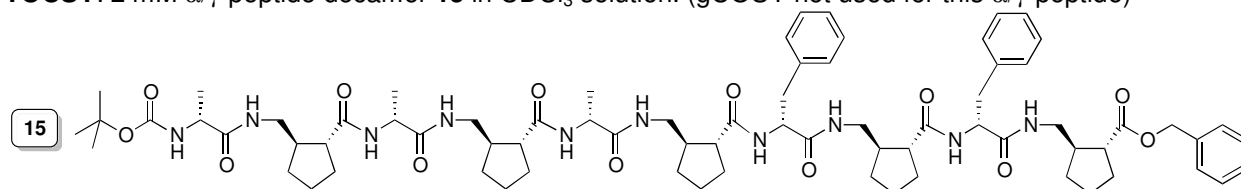




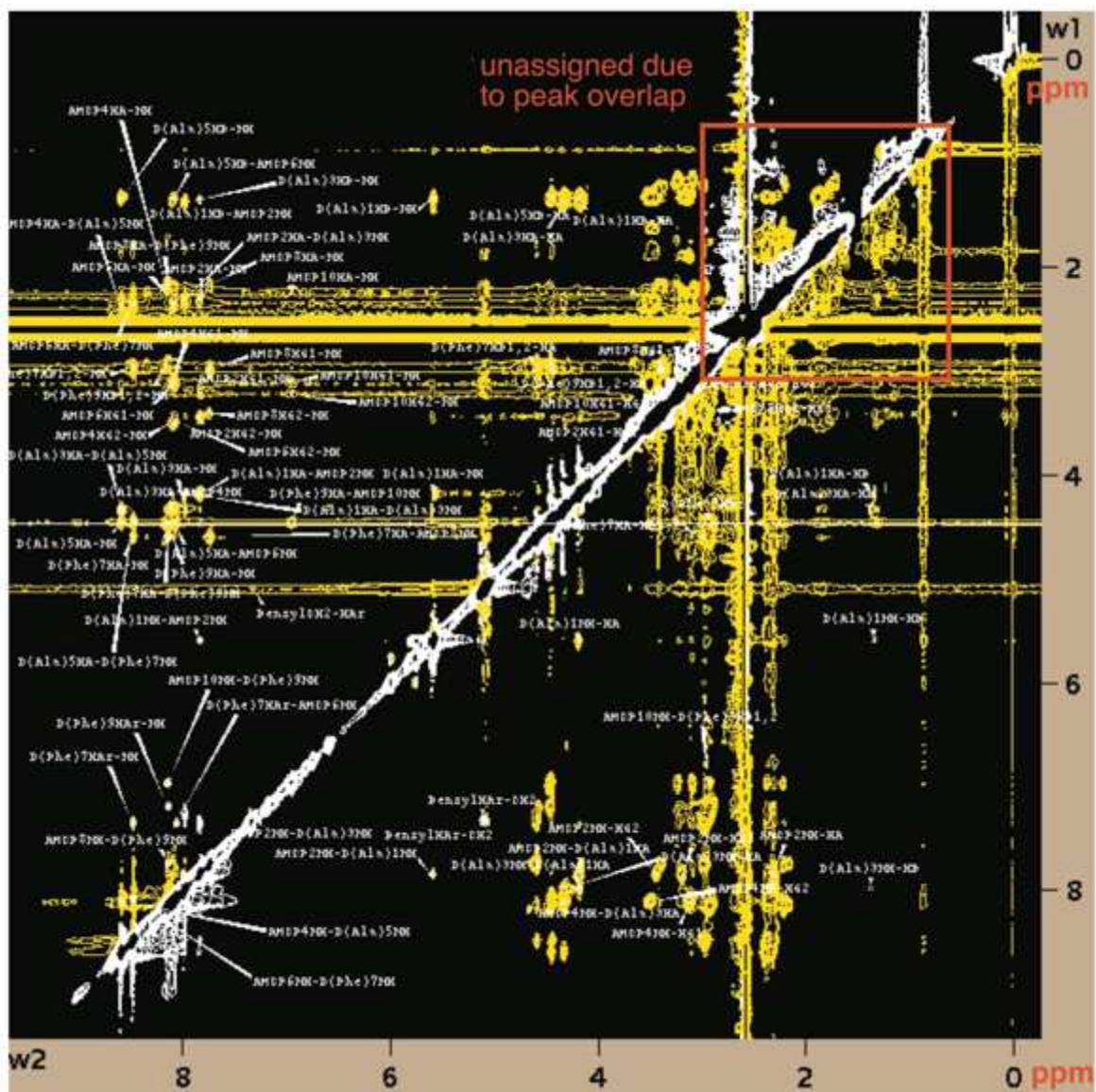
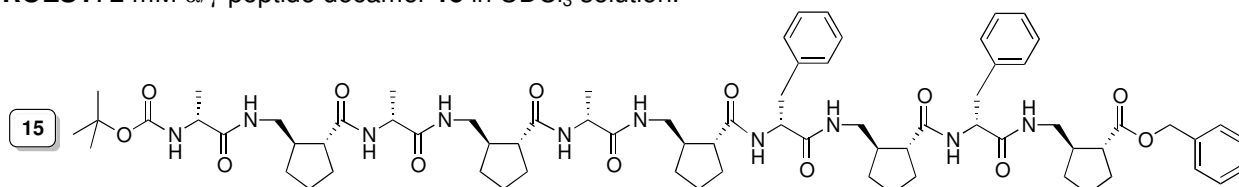
**Partial overlay of gCOSY, TOCSY, and ROESY used for assignment:** 2 mM  $\alpha/\gamma$ -peptide octamer **12** in  $\text{CDCl}_3$  solution. Positive ROESY peaks in gold, negative ROESY peaks in white. TOCSY peaks are in green.



**TOCSY:** 2 mM  $\alpha/\gamma$ -peptide decamer **15** in  $\text{CDCl}_3$  solution. (gCOSY not used for this  $\alpha/\gamma$ -peptide)

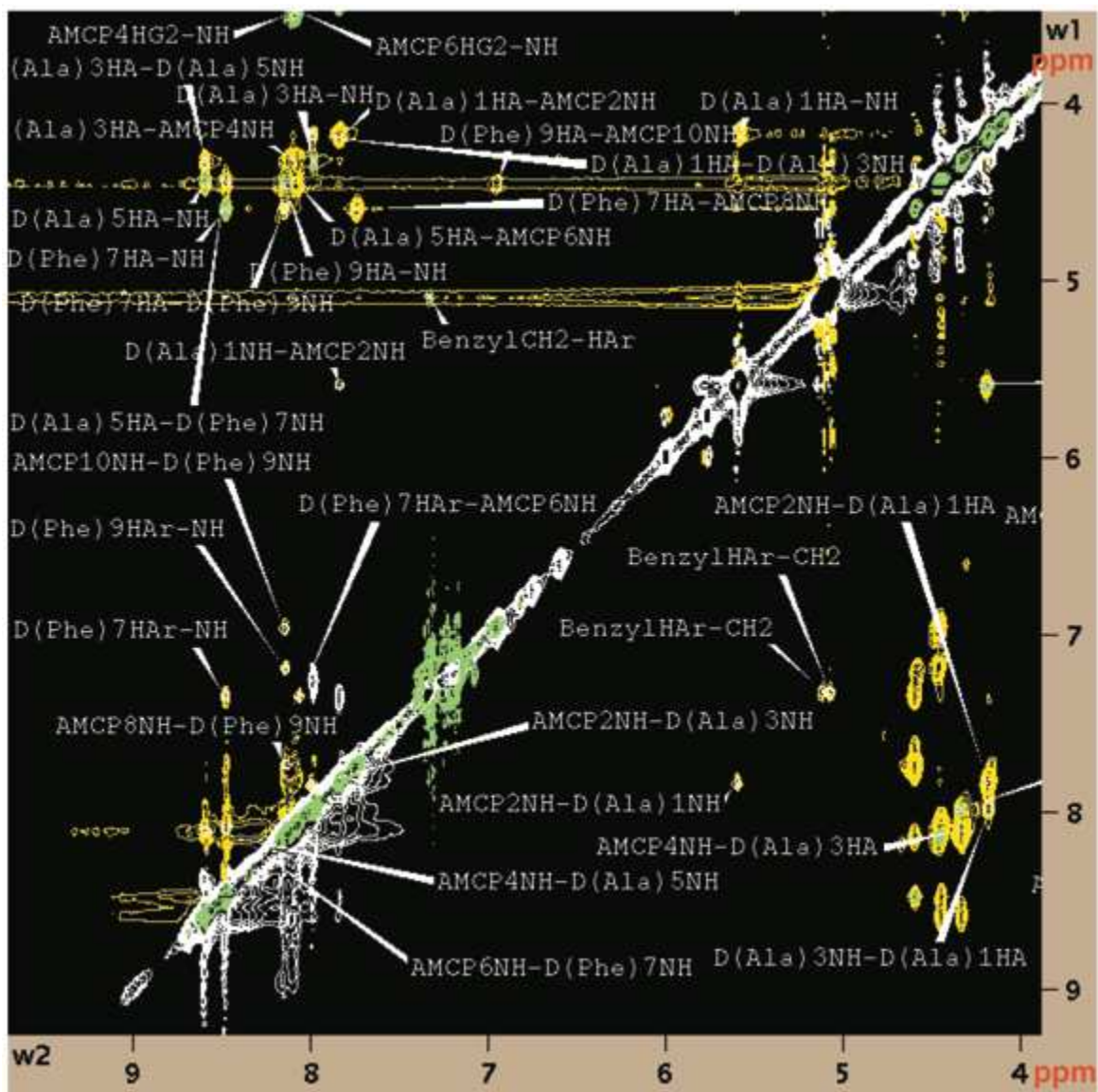
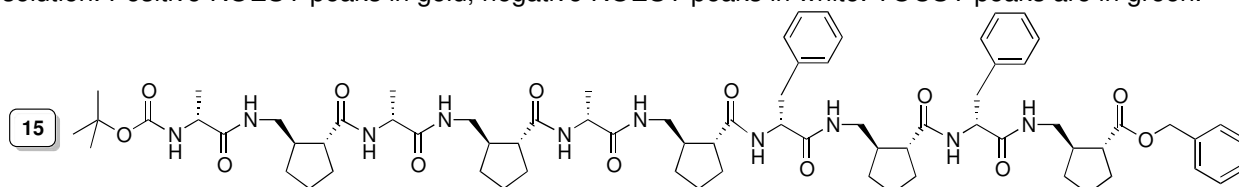


ROESY: 2 mM  $\alpha/\gamma$ -peptide decamer **15** in  $\text{CDCl}_3$  solution.



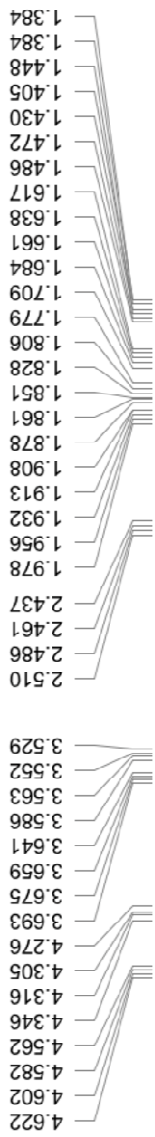
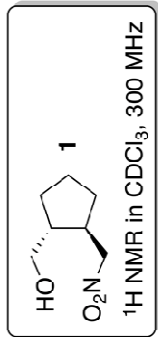
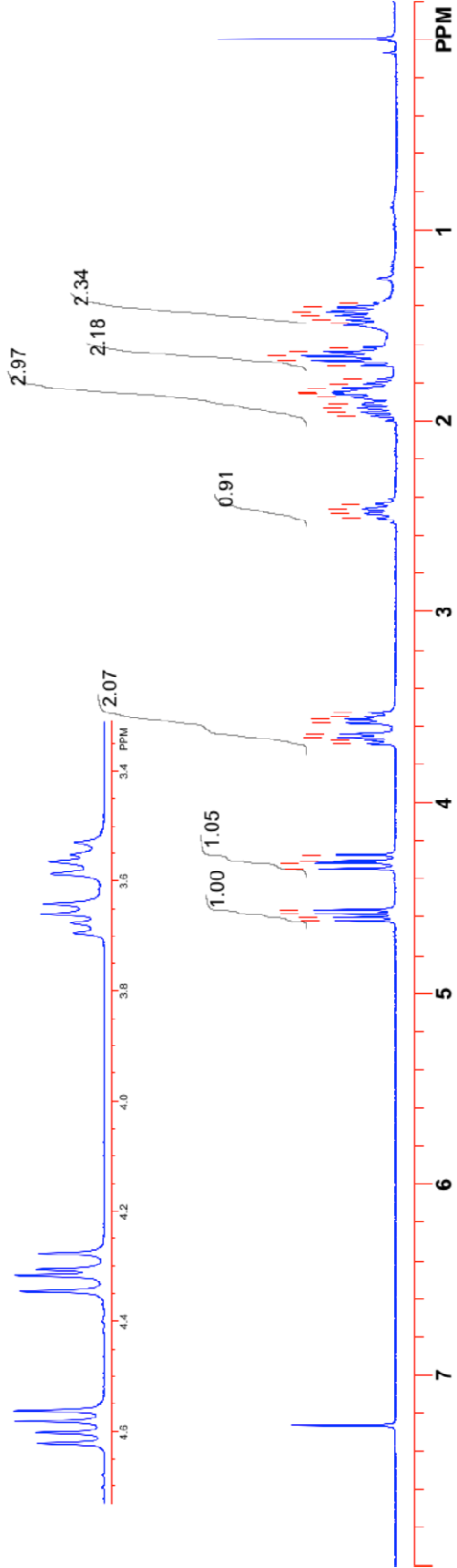


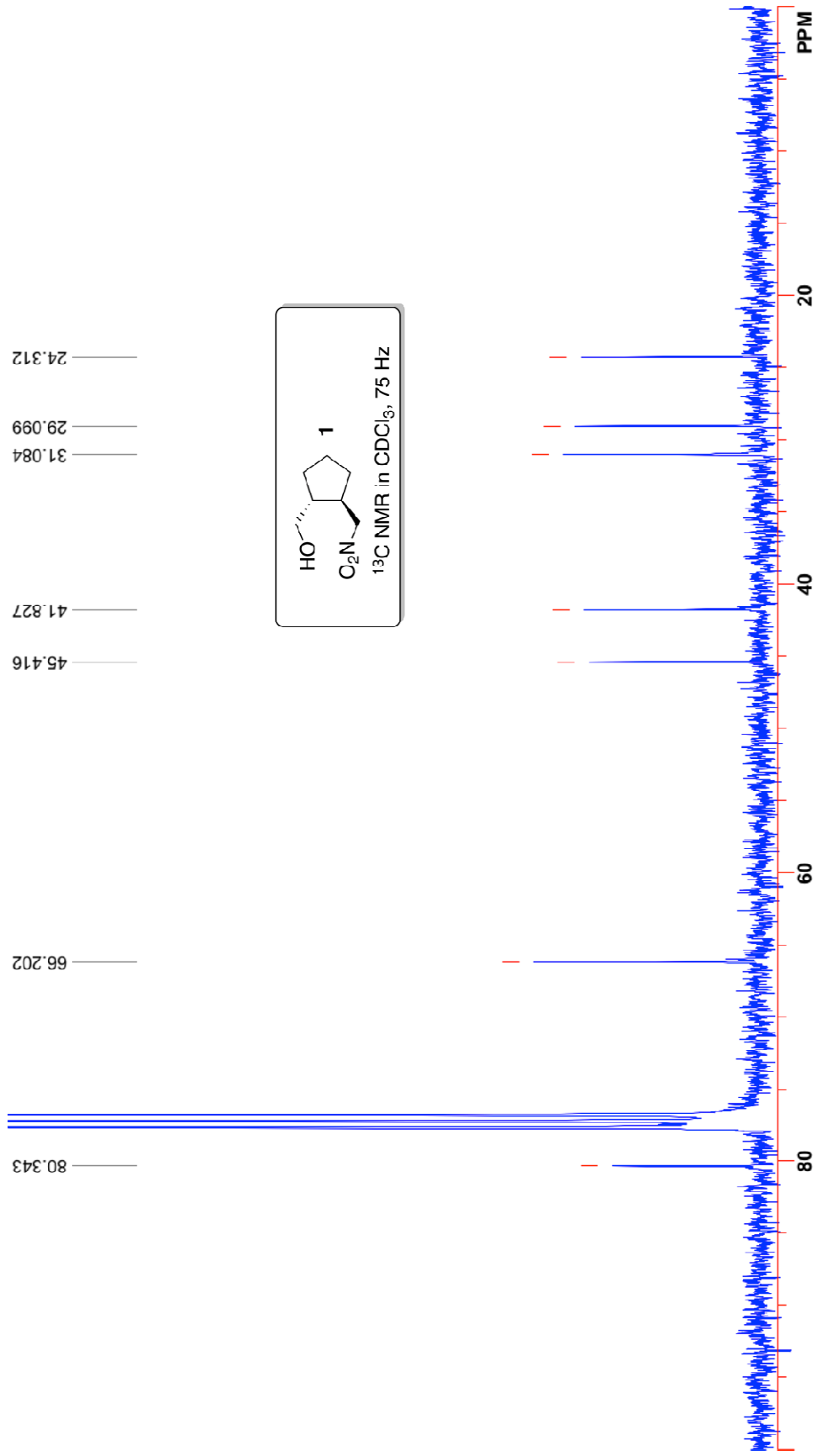
**Partial overlay of TOCSY and ROESY used for assignment:** 2 mM  $\alpha/\gamma$ -peptide decamer **15** in  $\text{CDCl}_3$  solution. Positive ROESY peaks in gold, negative ROESY peaks in white. TOCSY peaks are in green.

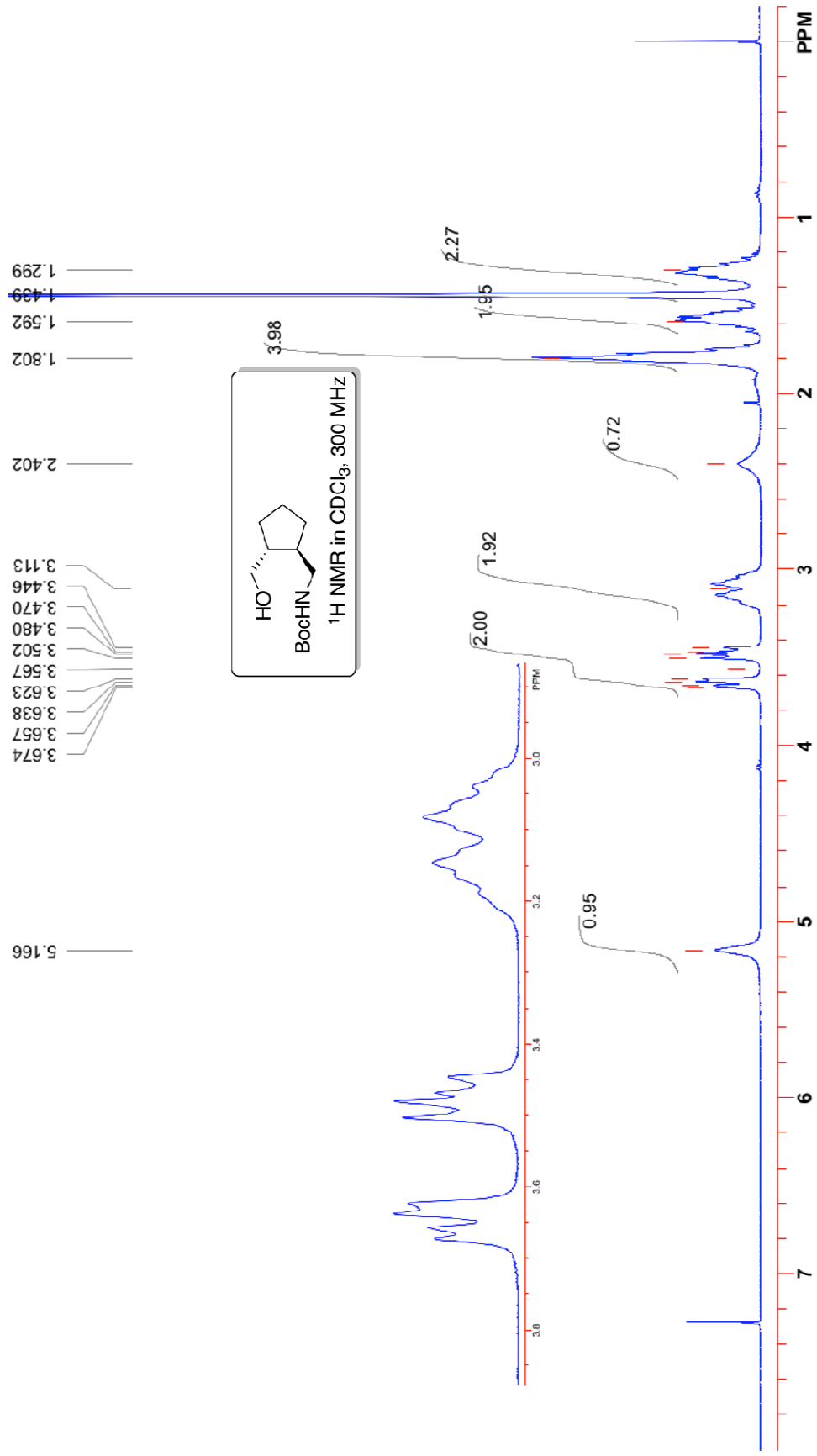


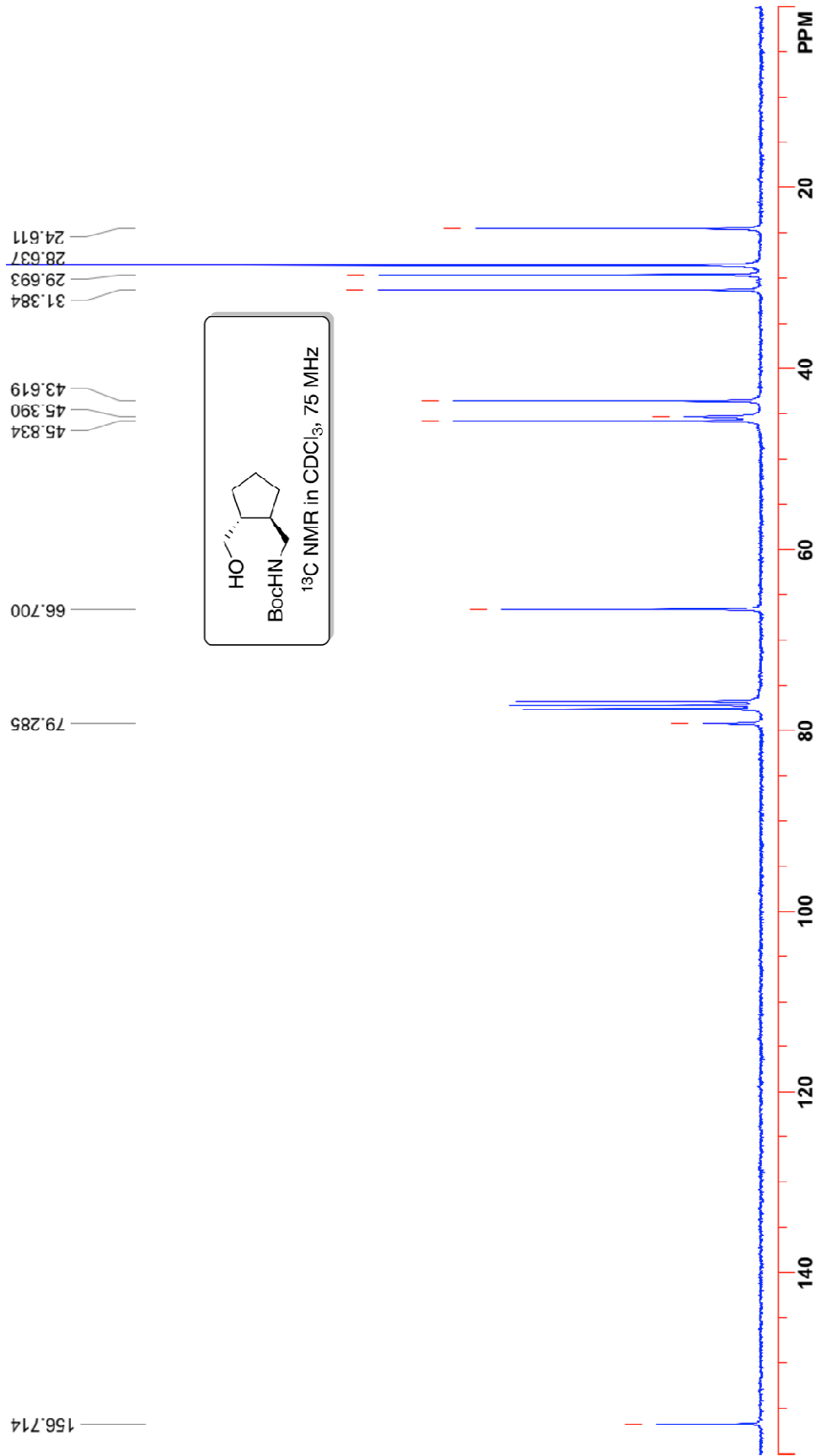


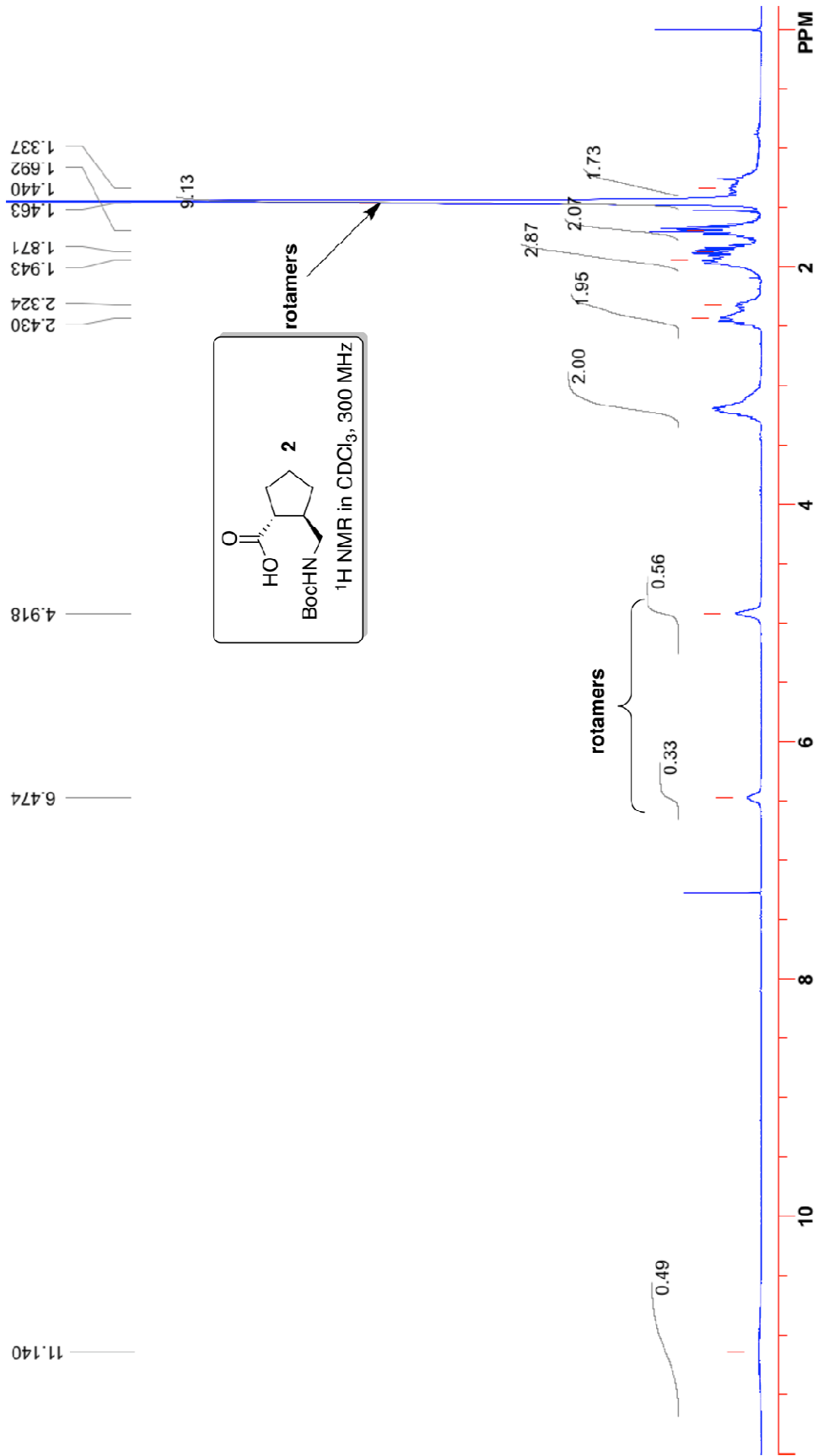
# **VII. 1D NMR Spectra for All New Compounds**

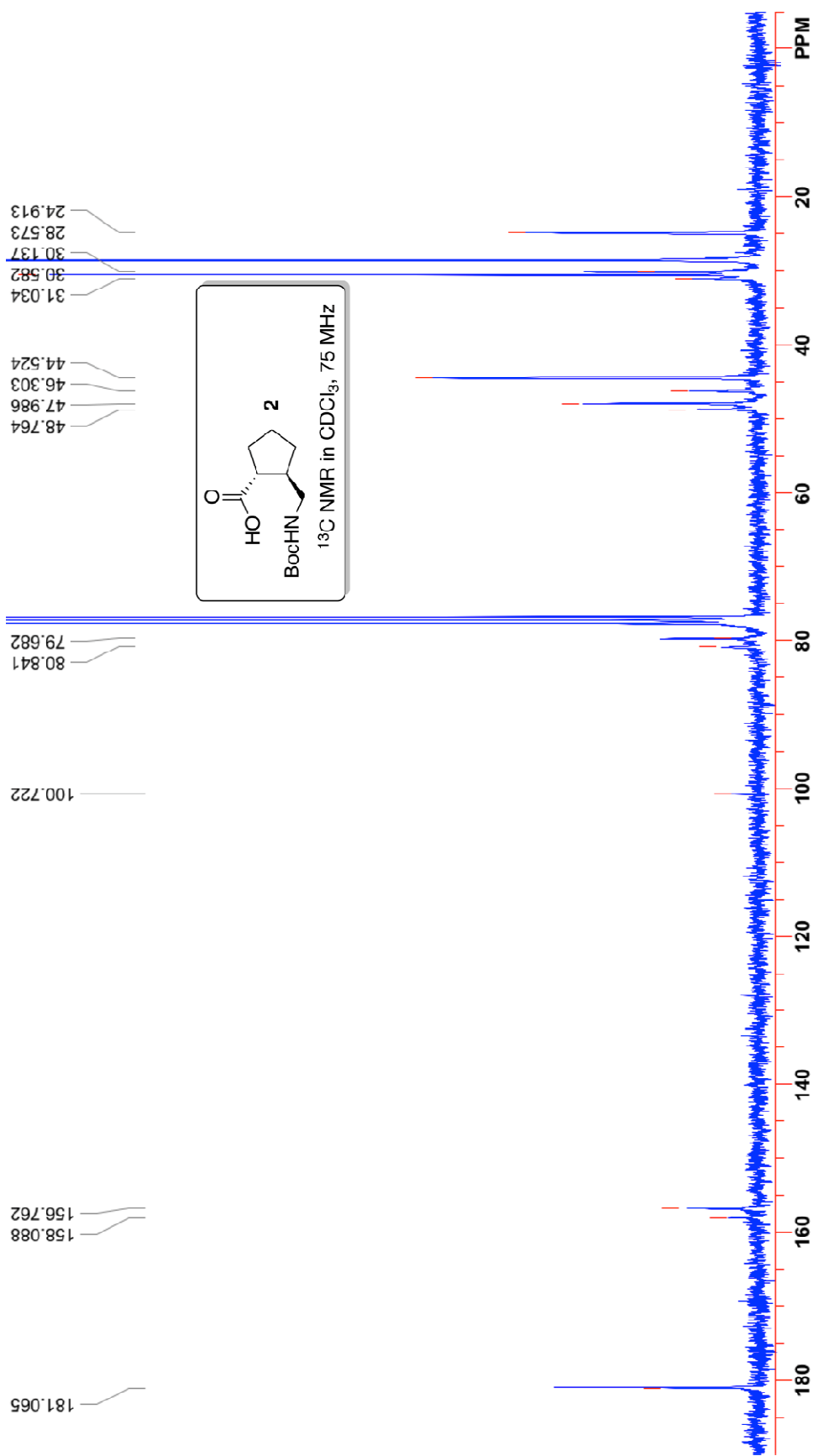


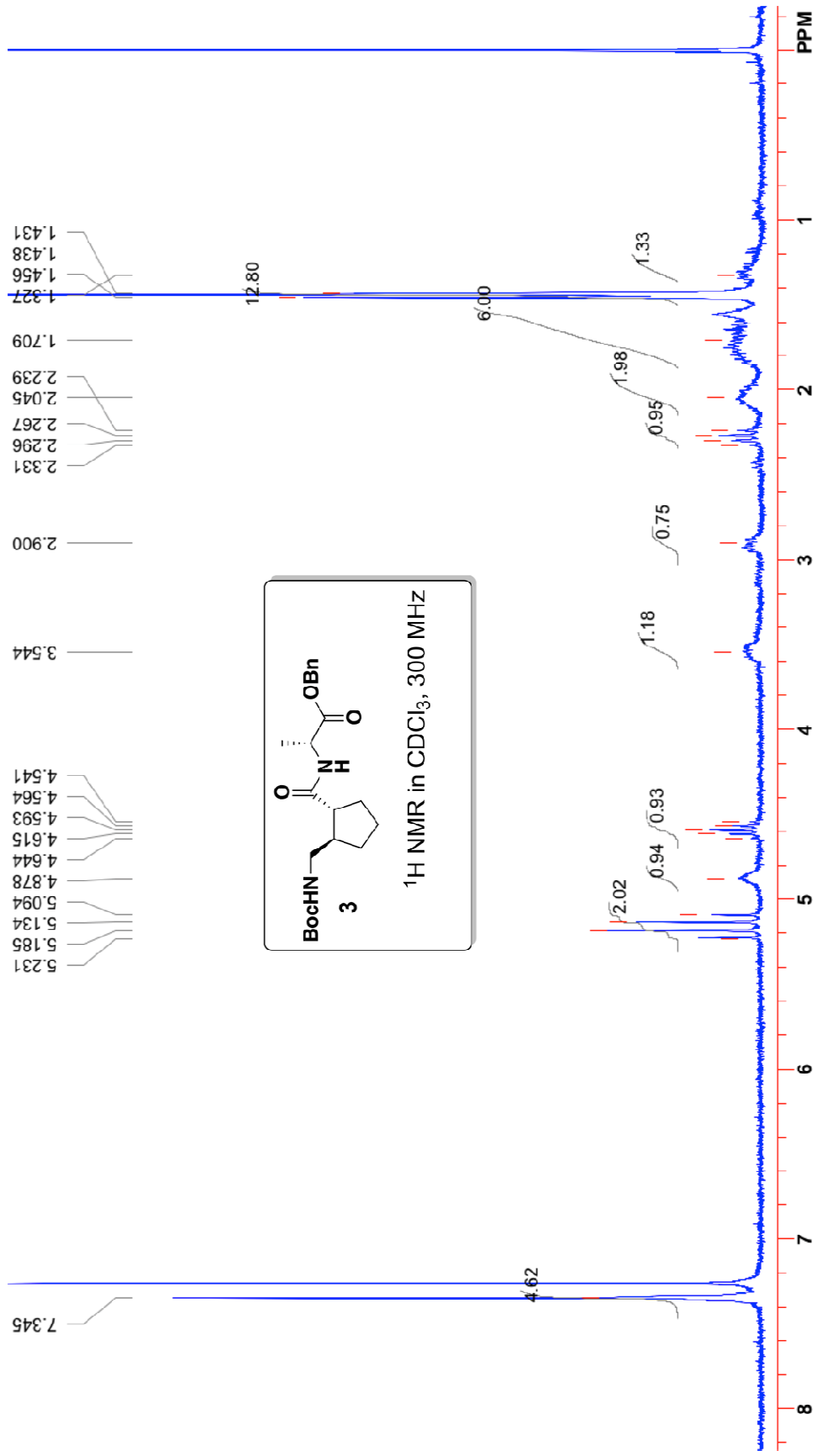




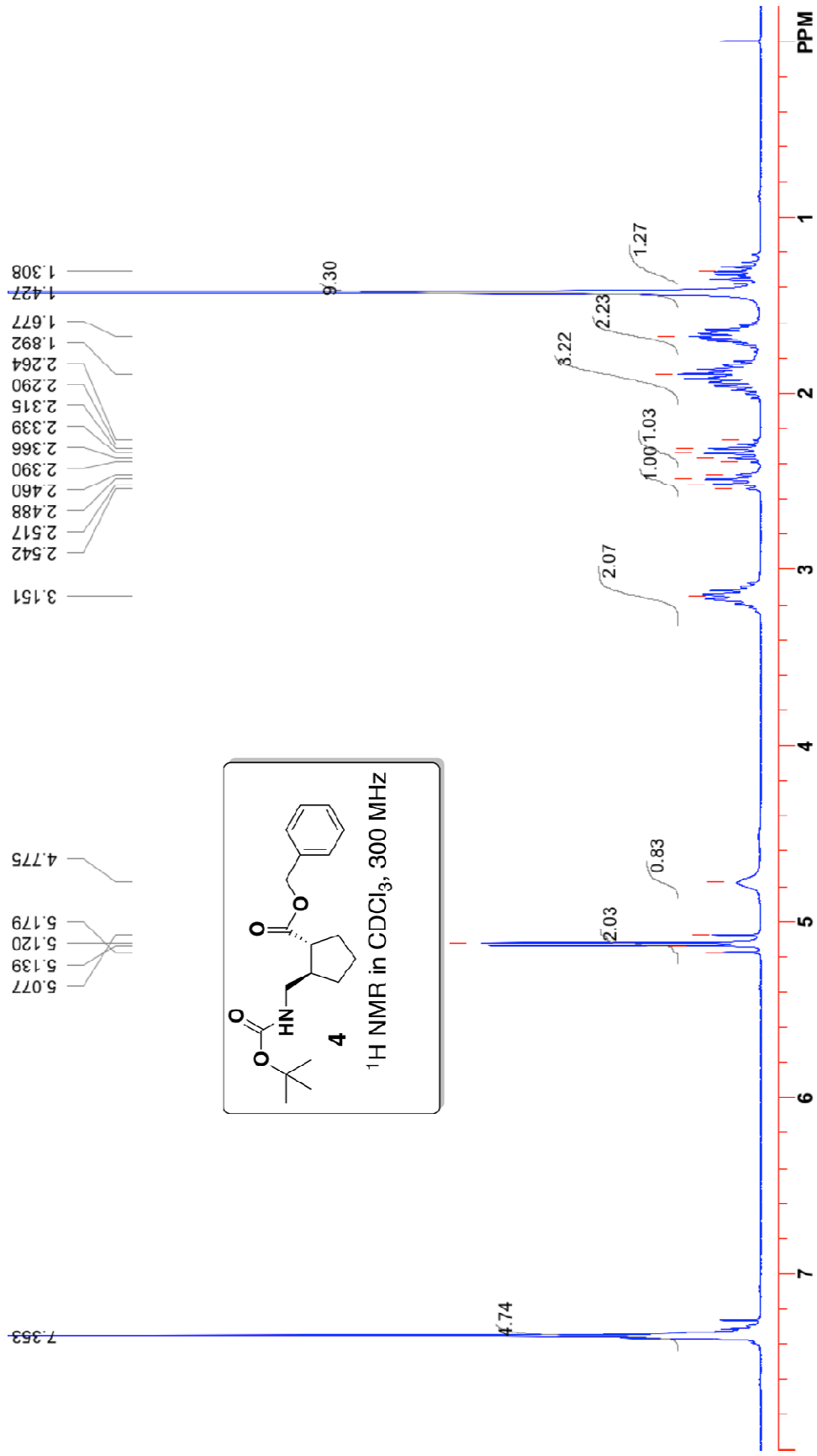


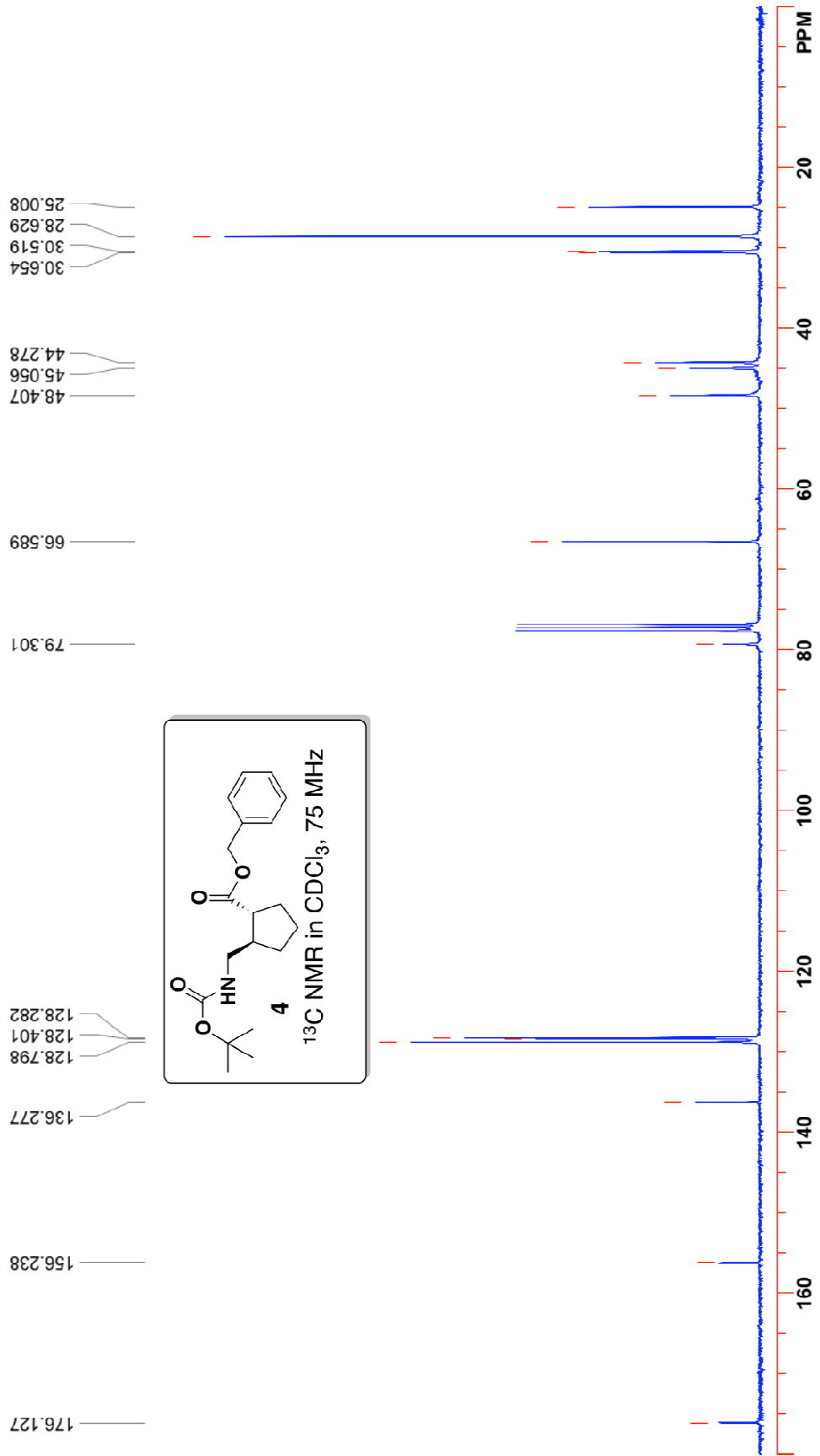


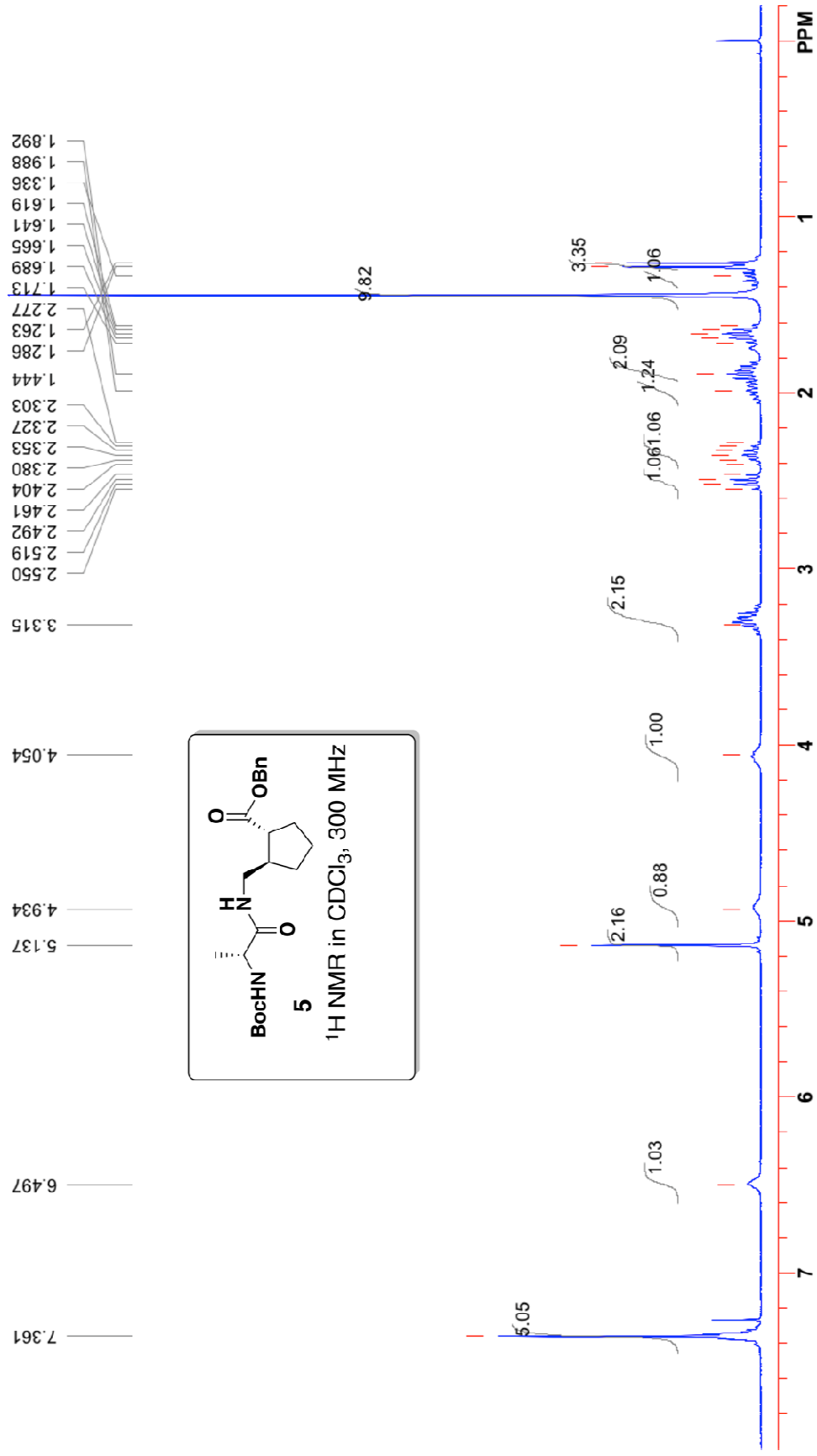


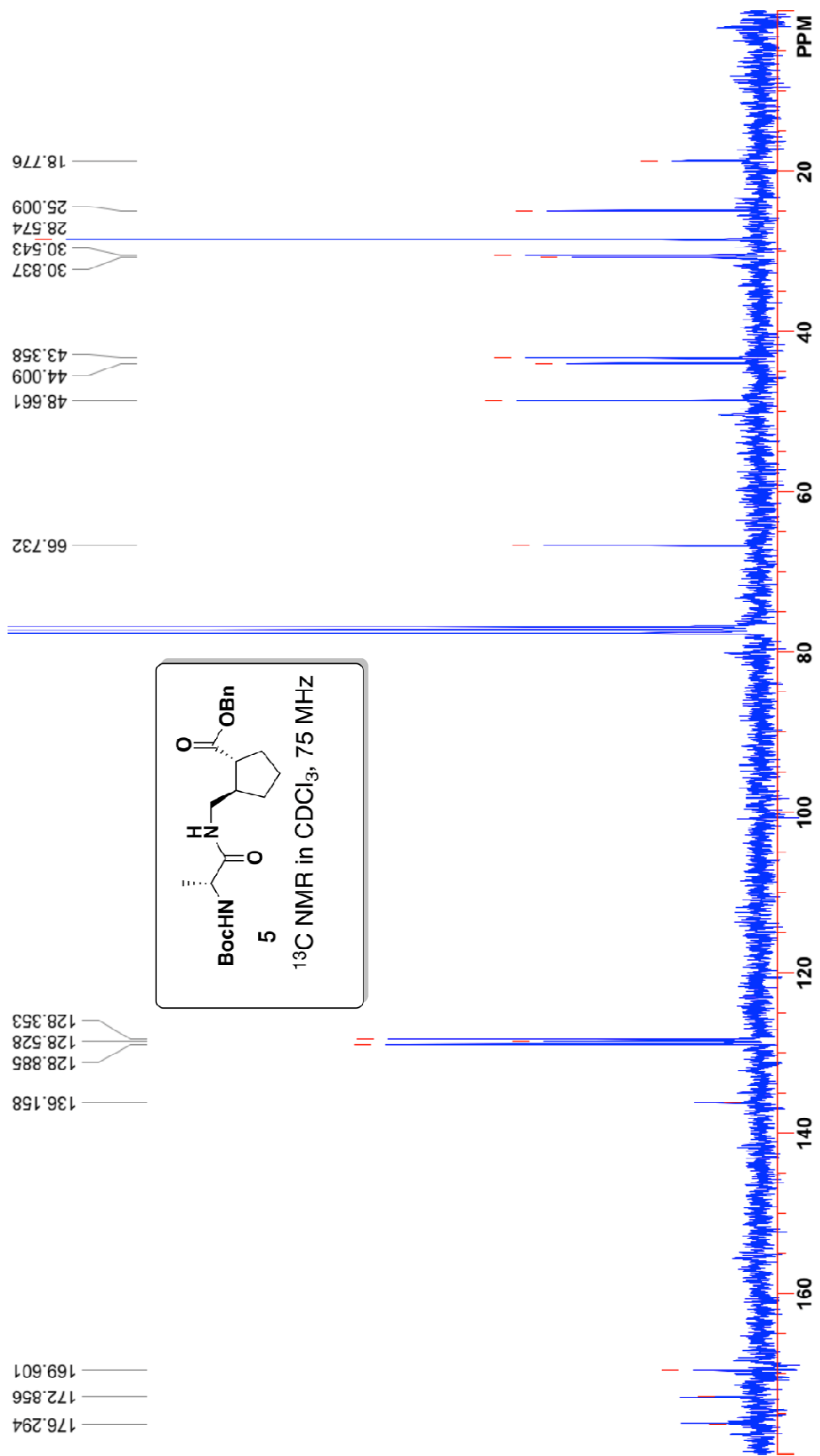


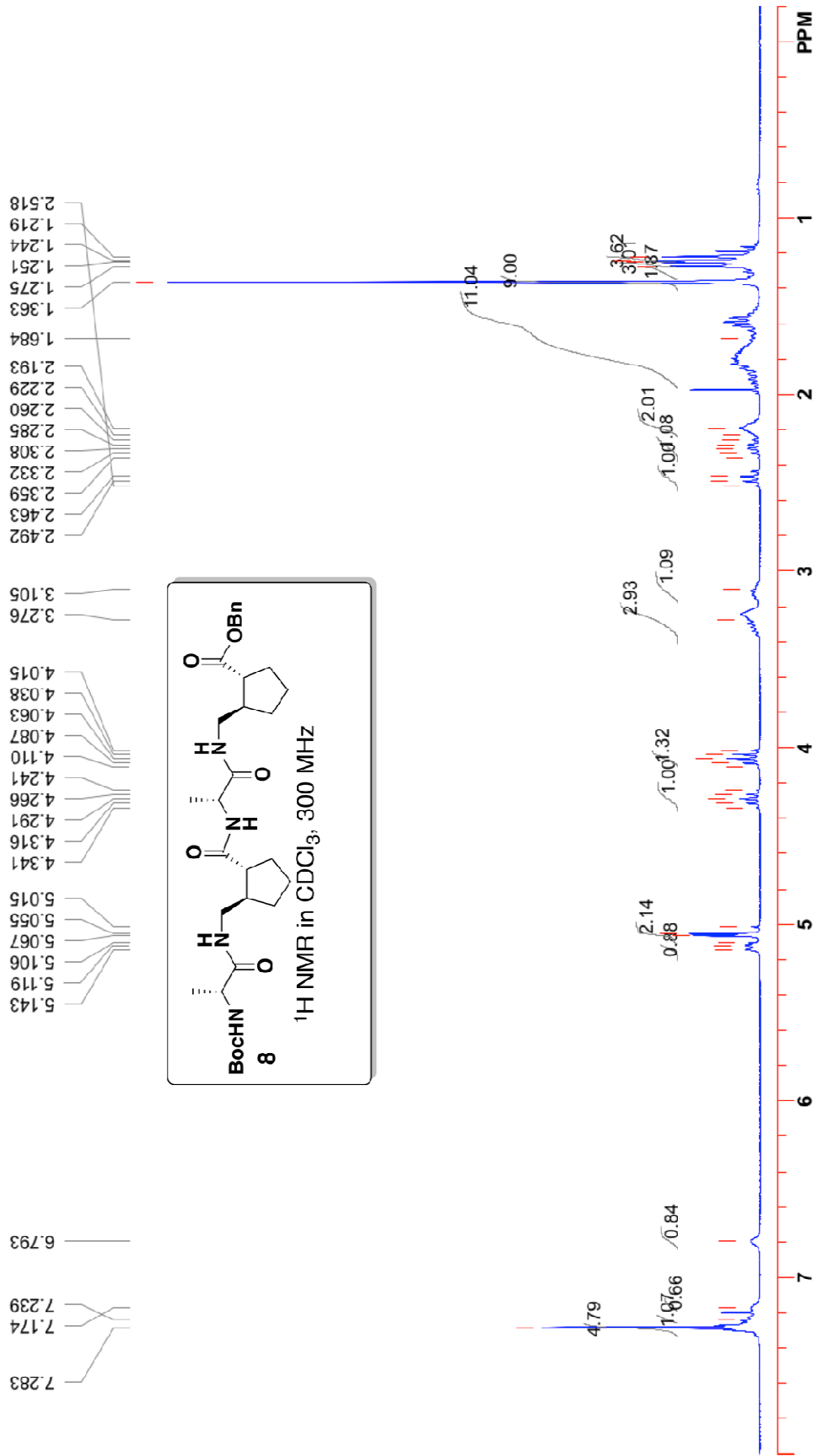


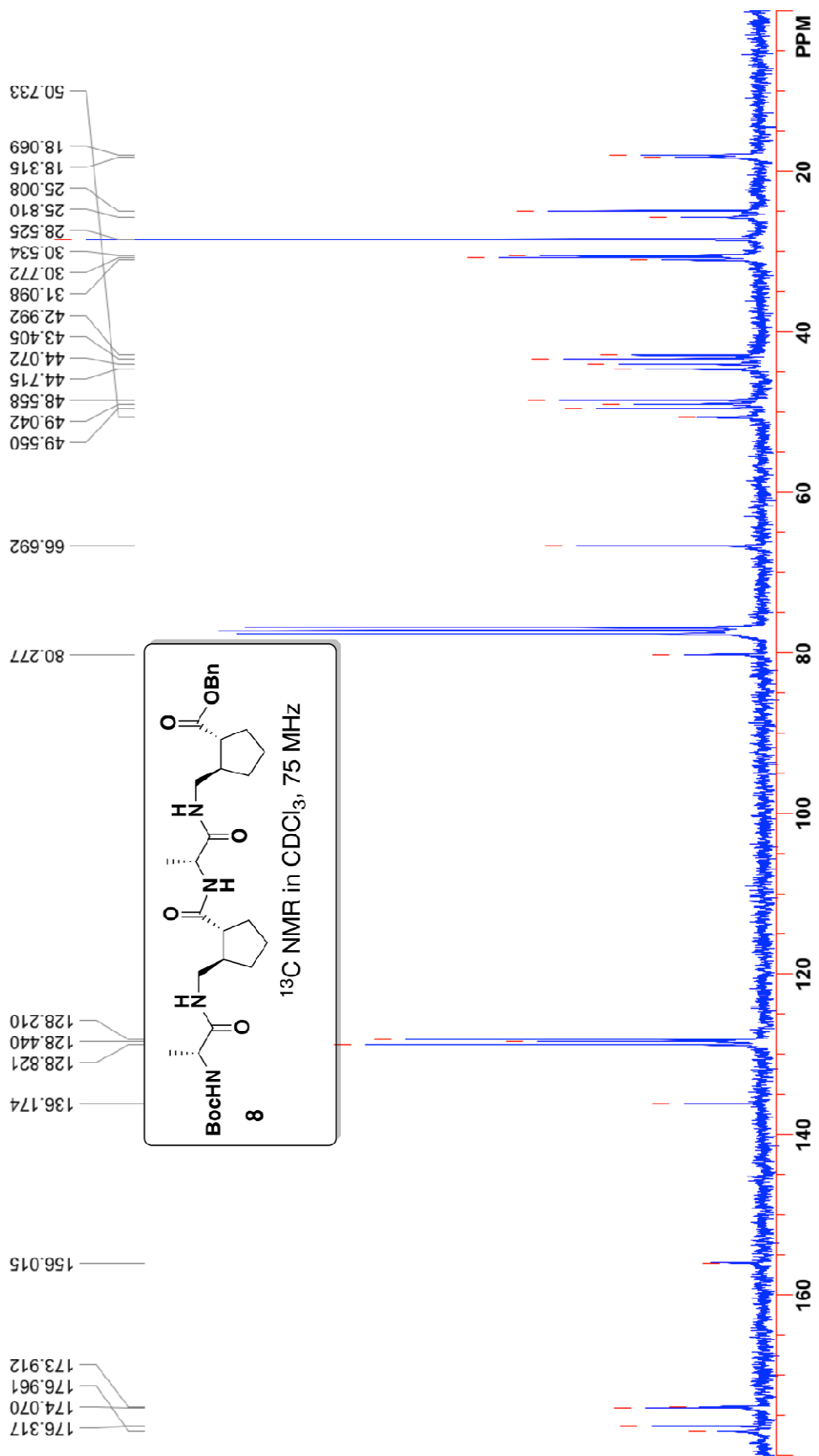


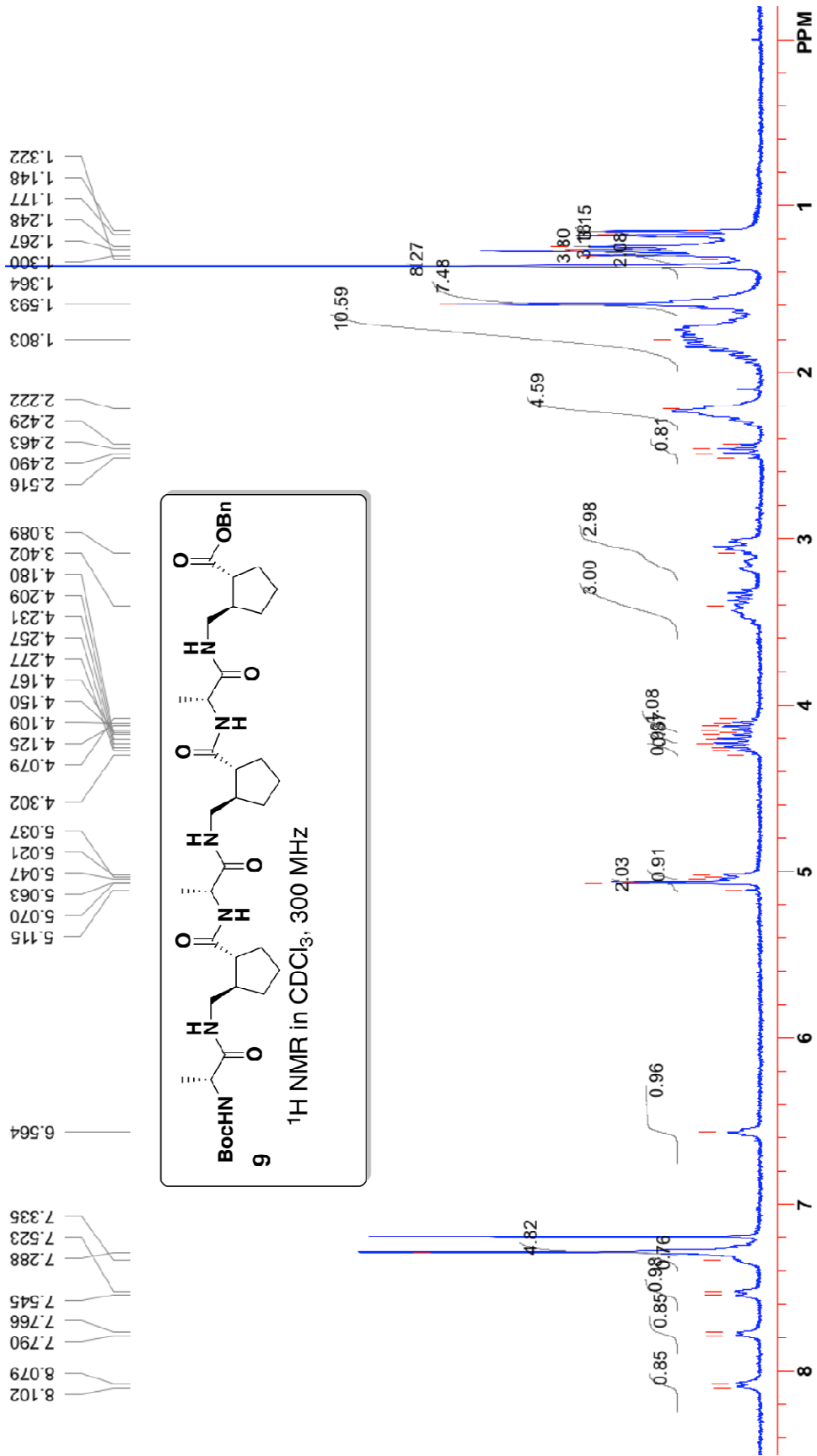


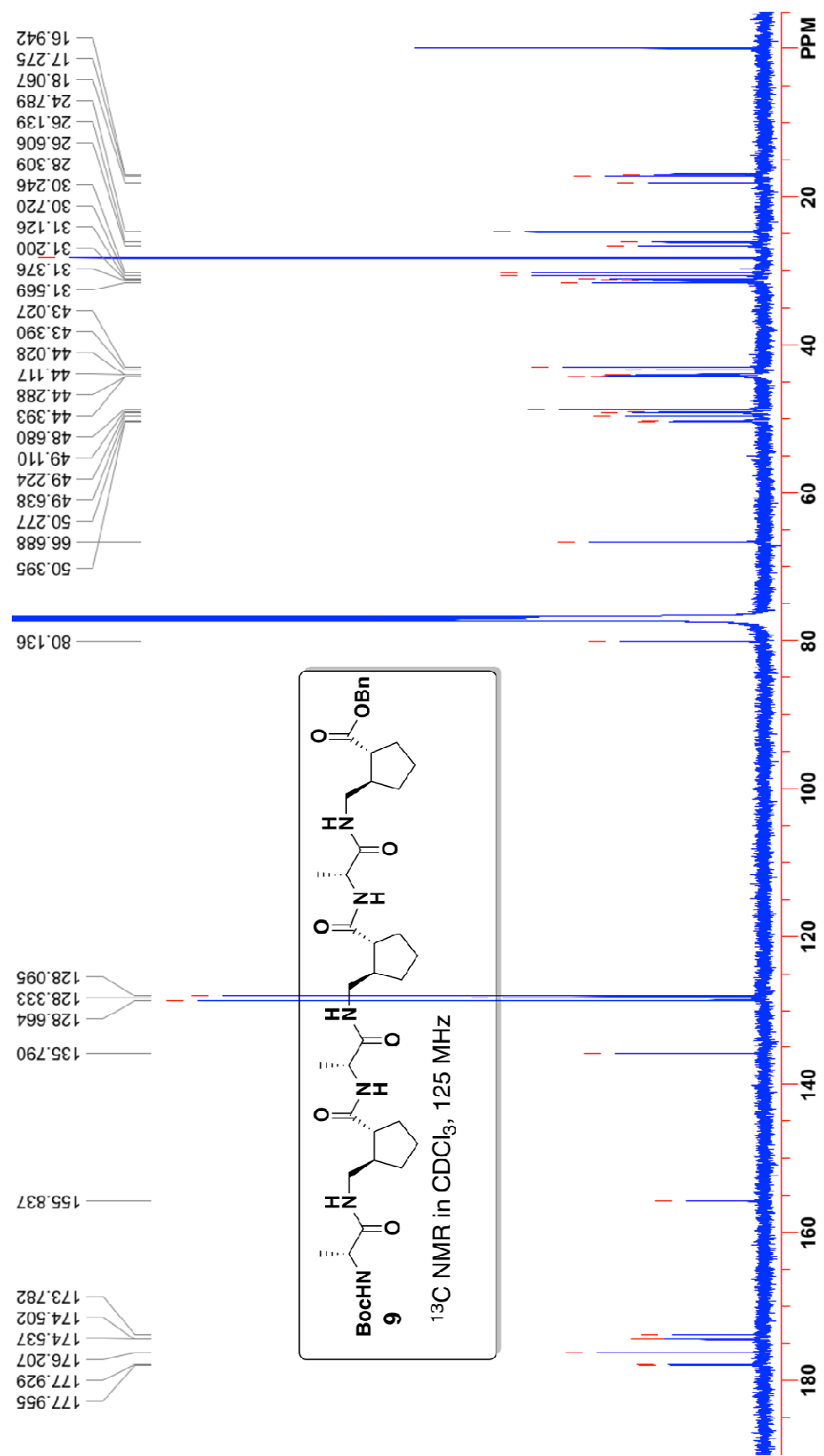








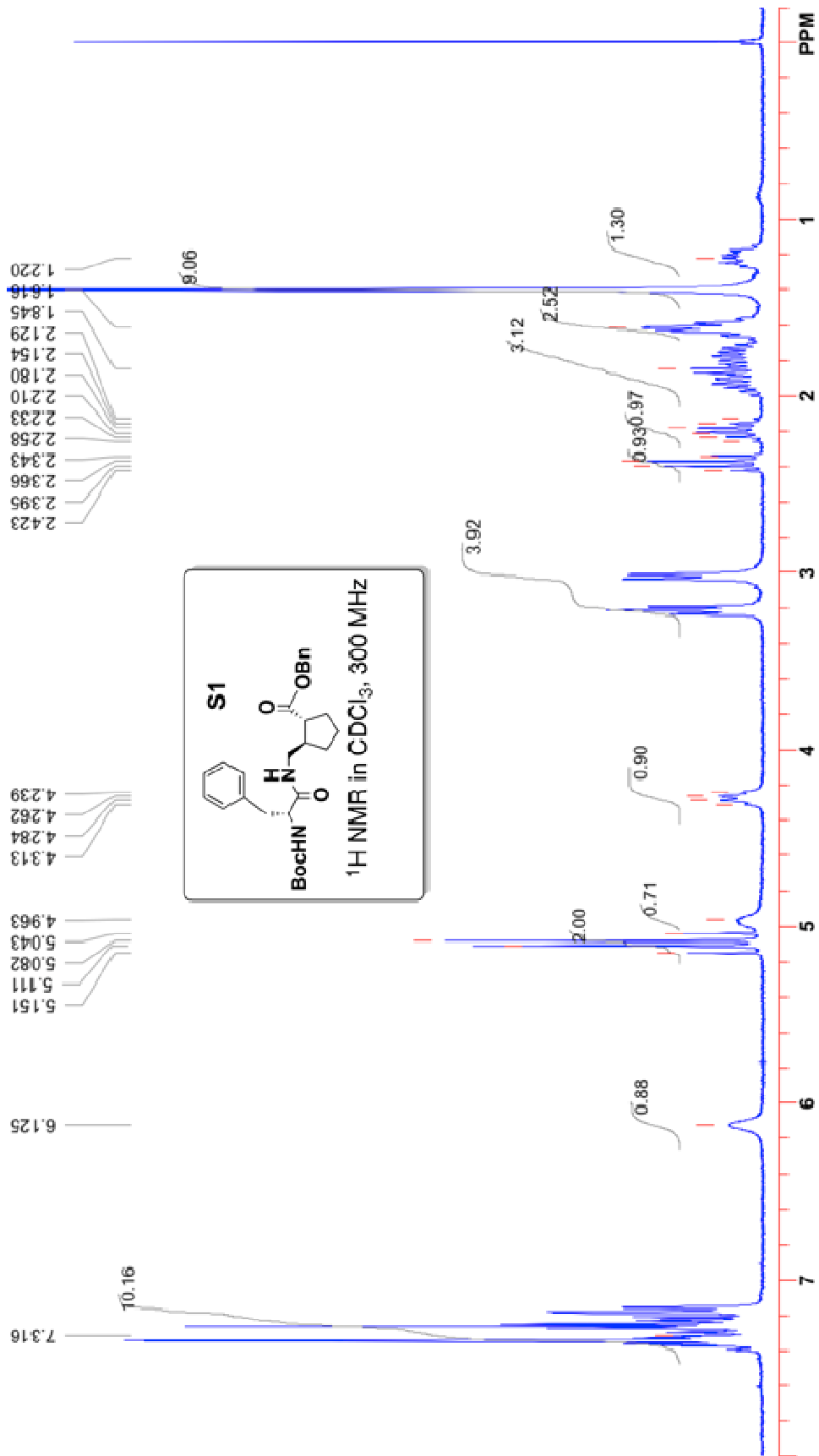


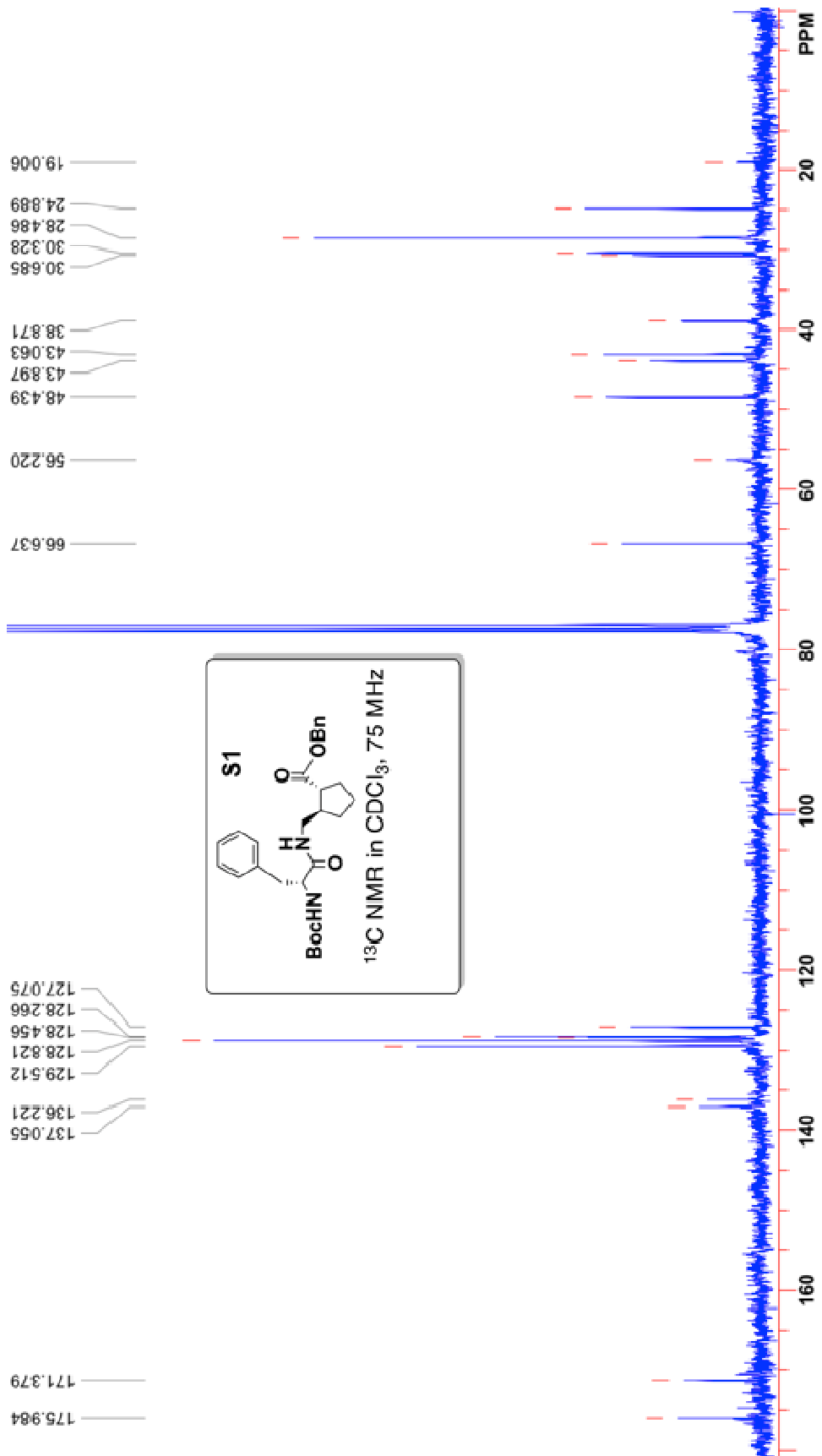


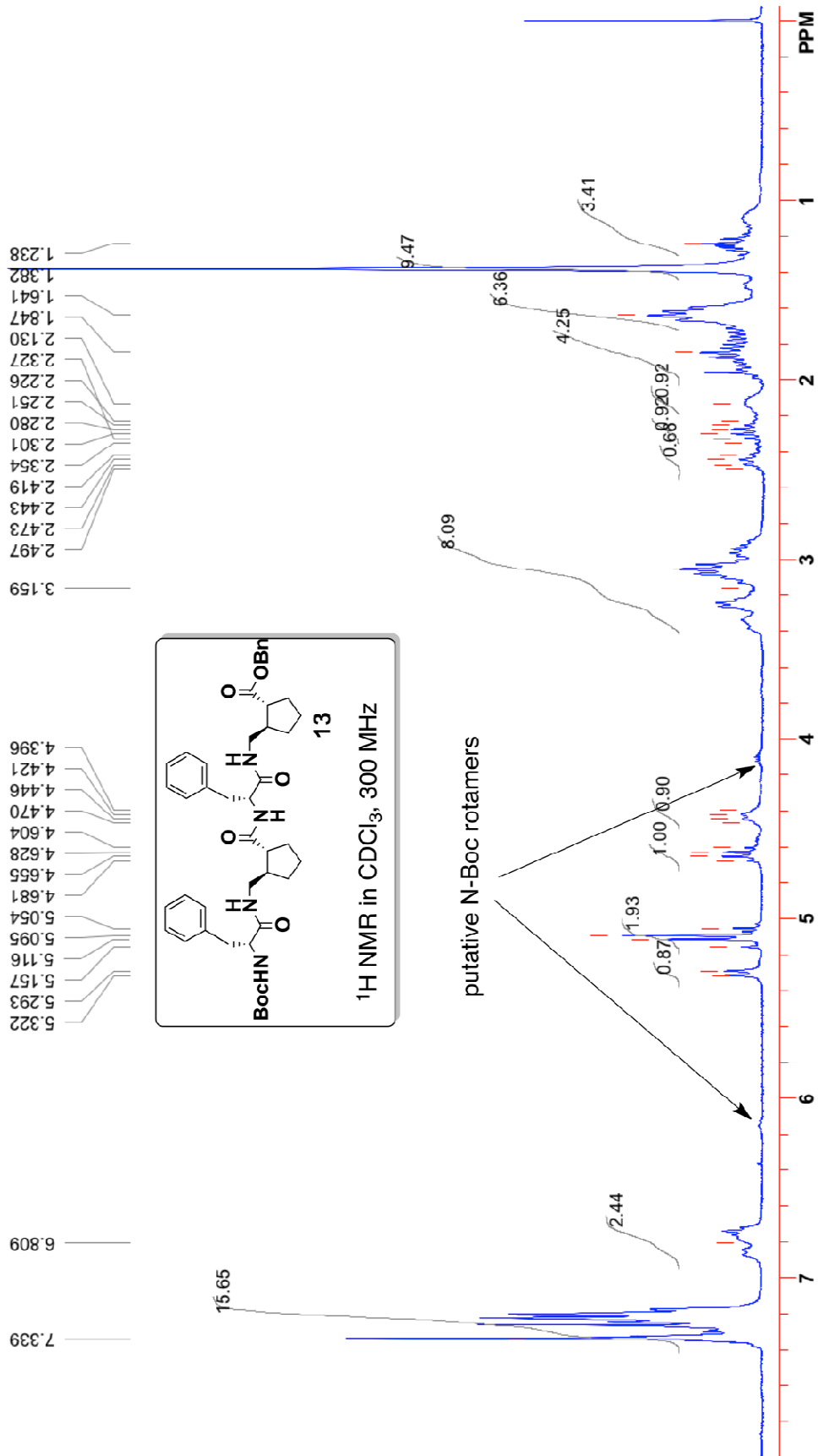


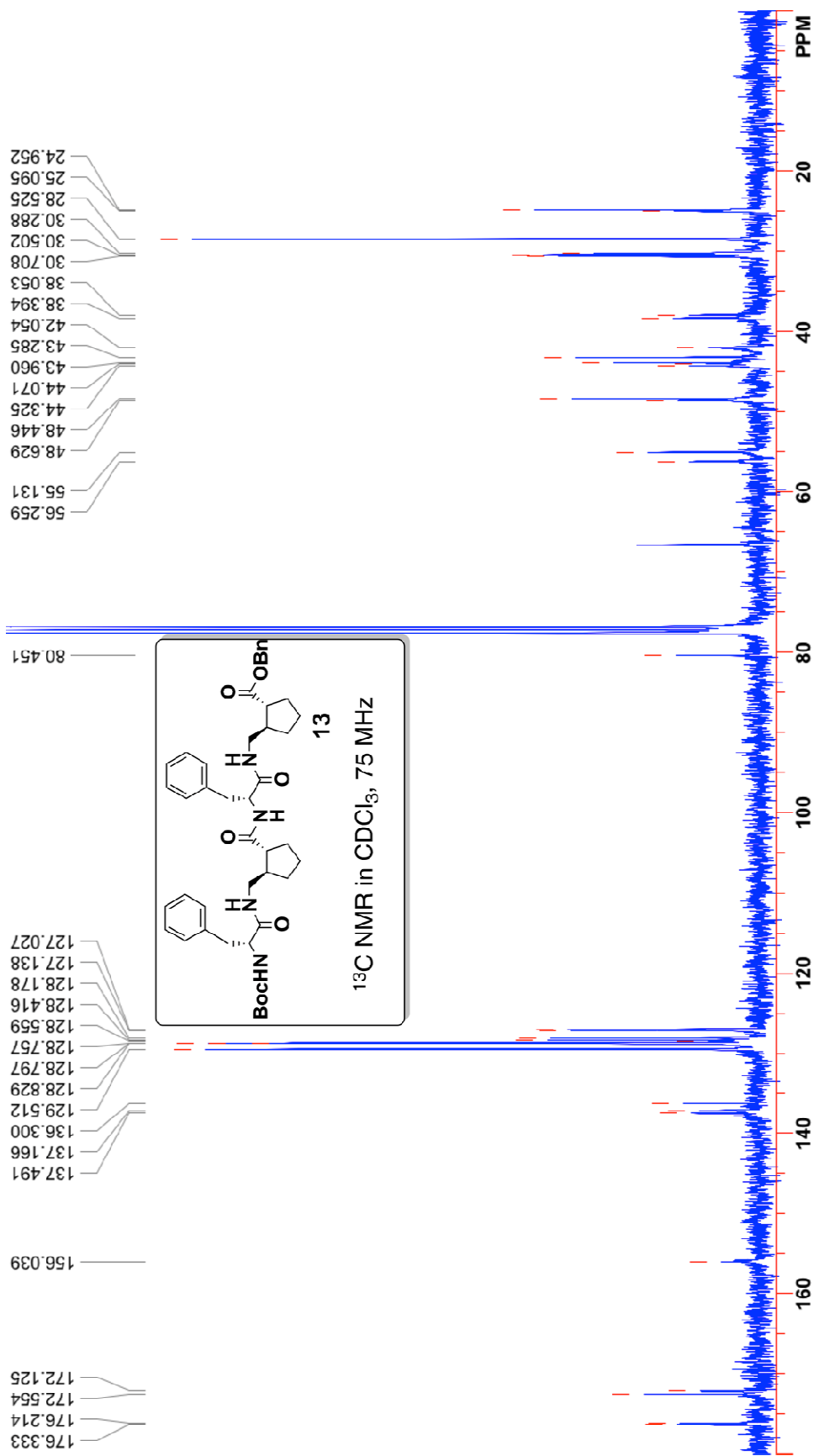


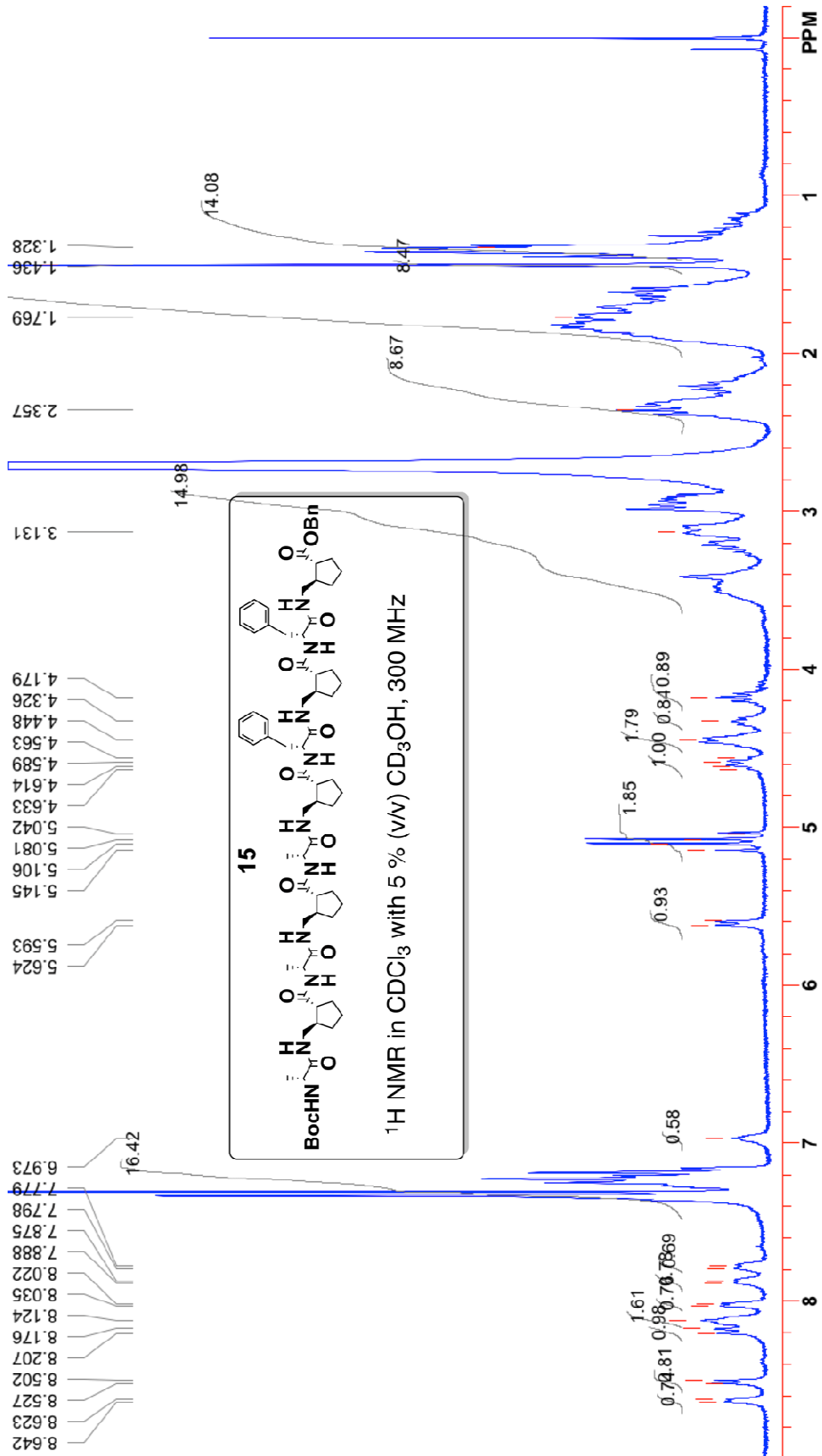


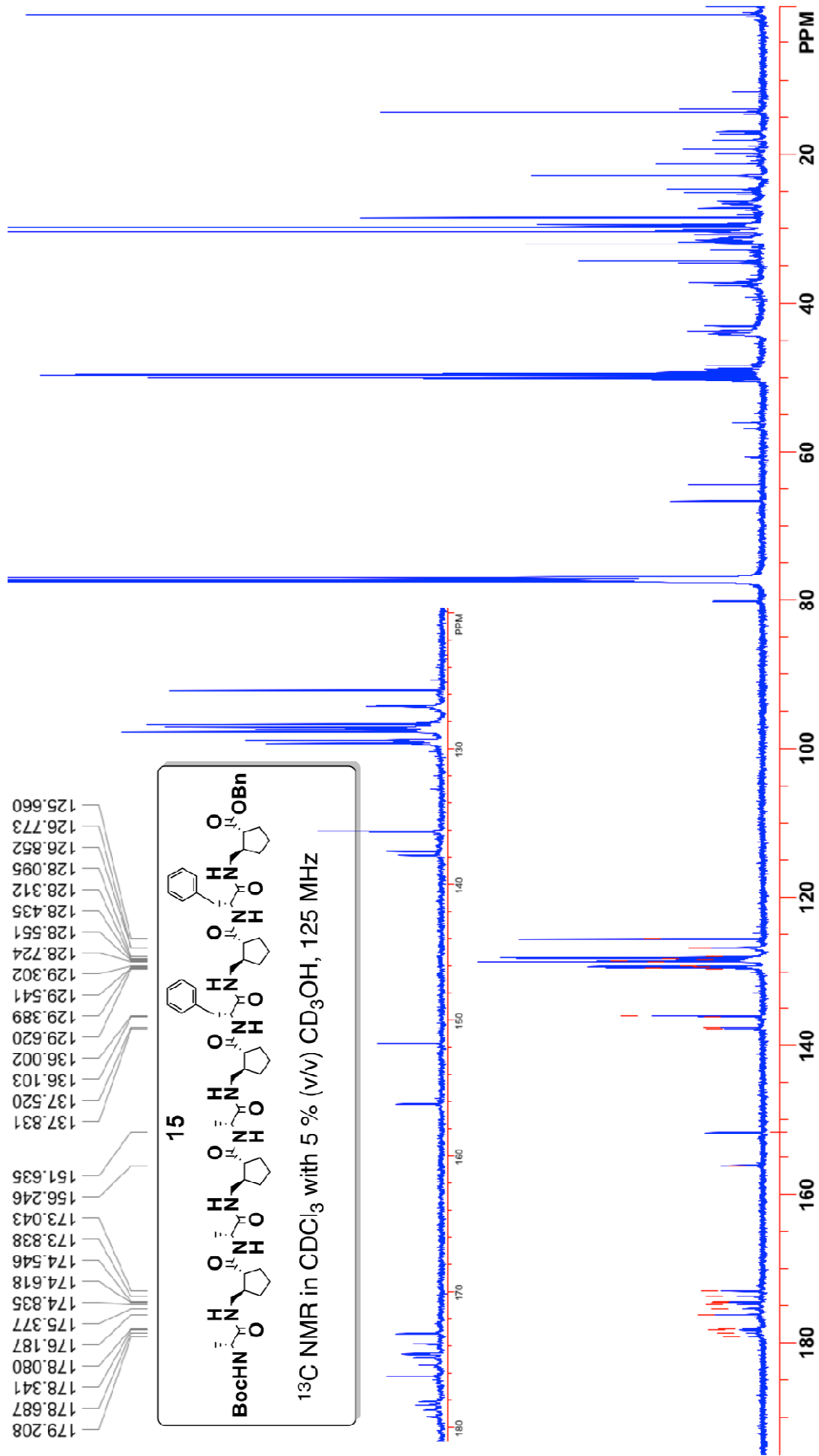














# **VIII. Crystallographic Report for Dipeptide 3**

## Crystallographic Experimental Section for Dipeptide **3** (gellman142)

Prepared by Ilia A. Guzei

### ***Data Collection***

A colorless crystal with dimensions 0.18 x 0.20 x 1.64 mm<sup>3</sup> was selected under oil under ambient conditions and attached to the tip of a MiTeGen MicroMount©. The crystal was mounted in a stream of cold nitrogen at 100(1) K and centered in the X-ray beam by using a video camera.

The crystal evaluation and data collection were performed on a Bruker SMART APEXII diffractometer with Cu K $\alpha$  ( $\lambda = 1.54178 \text{ \AA}$ ) radiation and the diffractometer to crystal distance of 4.03 cm.

The initial cell constants were obtained from three series of  $\omega$  scans at different starting angles. Each series consisted of 41 frames collected at intervals of 0.6° in a 25° range about  $\omega$  with the exposure time of 10 seconds per frame. The reflections were successfully indexed by an automated indexing routine built in the APEXII program. The final cell constants were calculated from a set of 9966 strong reflections from the actual data collection.

The data were collected by using the full sphere data collection routine to survey the reciprocal space to the extent of a full sphere to a resolution of 0.82 Å. A total of 11924 data were harvested by collecting 31 sets of frames with 0.85° scans in  $\omega$  with an exposure time 5-10 sec per frame. These highly redundant datasets were corrected for Lorentz and polarization effects. The absorption correction was based on fitting a function to the empirical transmission surface as sampled by multiple equivalent measurements. [1]

### **Structure Solution and Refinement**

The systematic absences in the diffraction data were consistent for the space groups  $P\bar{1}$  and  $P1$ . The  $E$ -statistics strongly suggested the non-centrosymmetric space group  $P1$  that yielded chemically reasonable and computationally stable results of refinement [2-4].

A successful solution by the direct methods provided most non-hydrogen atoms from the *E*-map. The remaining non-hydrogen atoms were located in an alternating series of least-squares cycles and difference Fourier maps. All non-hydrogen atoms were refined with anisotropic displacement coefficients. All non-amido hydrogen atoms were included in the structure factor calculation at idealized positions and were allowed to ride on the neighboring atoms with relative isotropic displacement coefficients. The amido hydrogen atoms were located in the difference map and refined with restraints.

The three chiral centers in the molecule are in the R configuration.

The final least-squares refinement of 275 parameters against 3389 data resulted in residuals *R* (based on  $F^2$  for  $I \geq 2\sigma$ ) and *wR* (based on  $F^2$  for all data) of 0.0307 and 0.0805, respectively. The final difference Fourier map was featureless.

The molecular diagram is drawn with 50% probability ellipsoids.

## References

- [1] Bruker-AXS. (2007) APEX2, SADABS, and SAINT Software Reference Manuals. Bruker-AXS, Madison, Wisconsin, USA.
- [2] Sheldrick, G. M. (2008) SHELXL. *Acta Cryst.* **A64**, 112-122.
- [3] Dolomanov, O.V.; Bourhis, L.J.; Gildea, R.J.; Howard, J.A.K.; Puschmann, H. "OLEX2: a complete structure solution, refinement and analysis program". *J. Appl. Cryst.* (2009) **42**, 339-341.
- [4] Guzei, I.A. (2006-2008). Internal laboratory computer programs "IG", "FCF\_filter", "Modicifer".

Figure 1. A molecular drawing of Gellman142.

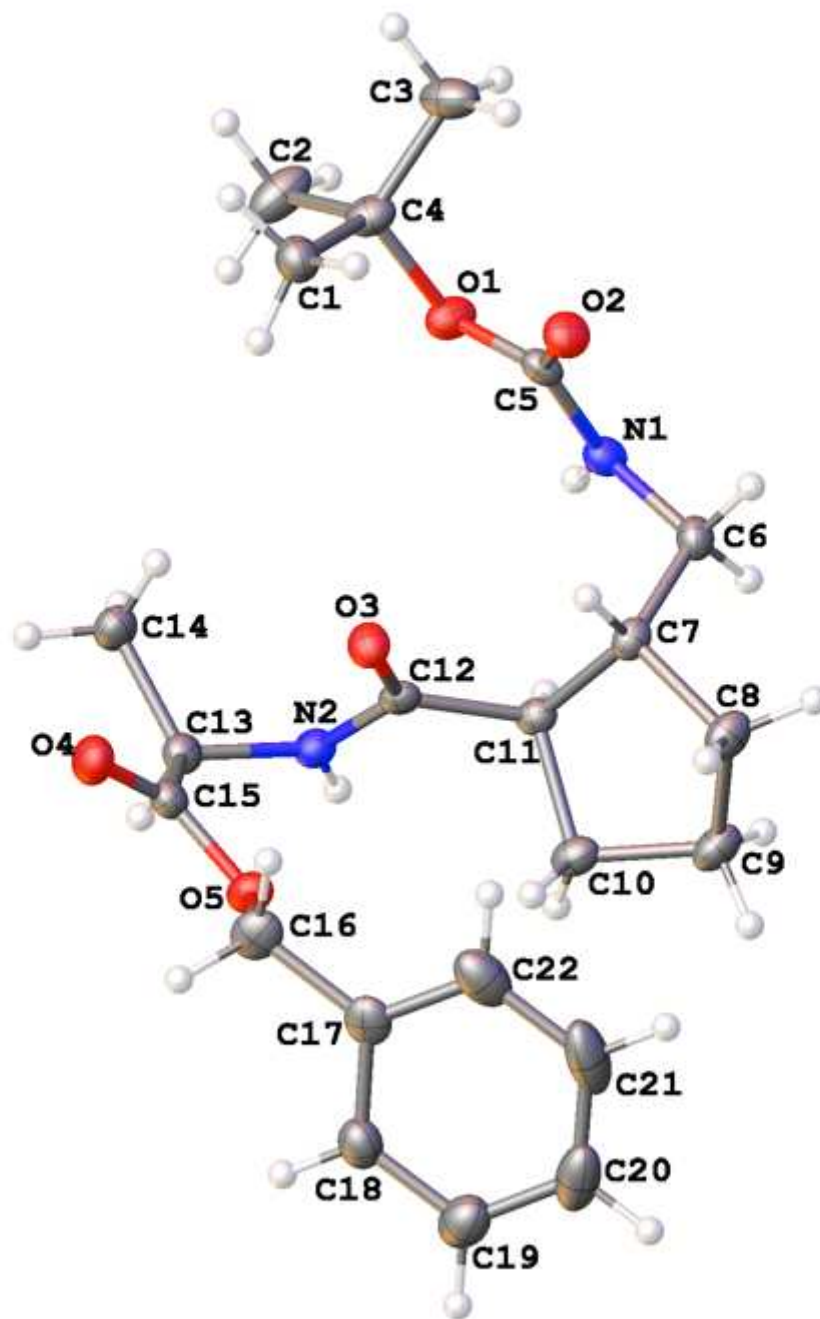


Table 1. Crystal data and structure refinement for gellman142.

Identification code	gellman142	
Empirical formula	C <sub>22</sub> H <sub>32</sub> N <sub>2</sub> O <sub>5</sub>	
Formula weight	404.50	
Temperature	100(1) K	
Wavelength	1.54178 Å	
Crystal system	Triclinic	
Space group	P1	
Unit cell dimensions	a = 5.041(3) Å	α = 92.56(3)°.
	b = 10.187(6) Å	β = 95.52(4)°.
	c = 10.943(7) Å	γ = 101.11(4)°.
Volume	547.7(5) Å <sup>3</sup>	
Z	1	
Density (calculated)	1.226 Mg/m <sup>3</sup>	
Absorption coefficient	0.706 mm <sup>-1</sup>	
F(000)	218	
Crystal size	1.64 x 0.20 x 0.18 mm <sup>3</sup>	
Theta range for data collection	4.07 to 69.46°.	
Index ranges	-6 ≤ h ≤ 5, -12 ≤ k ≤ 12, -13 ≤ l ≤ 13	
Reflections collected	11924	
Independent reflections	3389 [R(int) = 0.0187]	
Completeness to theta = 67.00°	97.5 %	
Absorption correction	Numerical with SADABS	
Max. and min. transmission	0.8835 and 0.3904	
Refinement method	Full-matrix least-squares on F <sup>2</sup>	
Data / restraints / parameters	3389 / 5 / 275	
Goodness-of-fit on F <sup>2</sup>	1.034	
Final R indices [I > 2σ(I)]	R1 = 0.0307, wR2 = 0.0803	
R indices (all data)	R1 = 0.0308, wR2 = 0.0805	
Absolute structure parameter Flack x	0.04(13)	
Absolute structure parameter Flack x	0.03(4)	
Largest diff. peak and hole	0.164 and -0.180 e.Å <sup>-3</sup>	

Table 2. Atomic coordinates ( $\times 10^4$ ) and equivalent isotropic displacement parameters ( $\text{\AA}^2 \times 10^3$ ) for gellman142.  $U(\text{eq})$  is defined as one third of the trace of the orthogonalized  $U^{ij}$  tensor.

	x	y	z	$U(\text{eq})$
O(1)	2417(2)	-610(1)	4589(1)	24(1)
O(2)	6033(2)	1075(1)	4376(1)	24(1)
O(3)	2604(2)	693(1)	966(1)	22(1)
O(4)	1609(2)	-1153(1)	-1613(1)	27(1)
O(5)	-95(2)	729(1)	-1519(1)	23(1)
N(1)	1756(3)	1452(1)	4388(1)	19(1)
N(2)	-1956(3)	116(1)	639(1)	18(1)
C(1)	5458(4)	-1796(2)	3544(1)	27(1)
C(2)	1902(4)	-2911(2)	4800(2)	38(1)
C(3)	6004(4)	-1367(2)	5879(2)	33(1)
C(4)	4051(3)	-1658(2)	4703(1)	25(1)
C(5)	3612(3)	670(2)	4436(1)	19(1)
C(6)	2408(3)	2831(1)	4042(1)	21(1)
C(7)	2592(3)	2922(1)	2660(1)	19(1)
C(8)	2889(4)	4384(2)	2284(2)	26(1)
C(9)	27(4)	4505(2)	1776(2)	28(1)
C(10)	-1030(3)	3167(2)	1042(1)	24(1)
C(11)	-33(3)	2145(1)	1898(1)	18(1)
C(12)	360(3)	917(1)	1148(1)	18(1)
C(13)	-1856(3)	-980(2)	-253(1)	21(1)
C(14)	-1160(4)	-2205(2)	360(1)	26(1)
C(15)	129(3)	-497(1)	-1191(1)	21(1)
C(16)	1915(4)	1364(2)	-2298(2)	29(1)
C(17)	1583(3)	2793(2)	-2347(1)	26(1)
C(18)	-535(4)	3128(2)	-3096(1)	29(1)
C(19)	-921(4)	4435(2)	-3100(2)	37(1)
C(20)	809(5)	5429(2)	-2352(2)	42(1)
C(21)	2918(5)	5125(2)	-1611(2)	46(1)
C(22)	3327(4)	3804(2)	-1607(2)	38(1)

Table 3. Bond lengths [Å] and angles [°] for gellman142.

O(1)-C(5)	1.3519(19)	C(8)-H(8B)	0.9900
O(1)-C(4)	1.472(2)	C(8)-H(8A)	0.9900
O(2)-C(5)	1.220(2)	C(9)-C(10)	1.526(2)
O(3)-C(12)	1.229(2)	C(9)-H(9B)	0.9900
O(4)-C(15)	1.203(2)	C(9)-H(9A)	0.9900
O(5)-C(15)	1.3375(19)	C(10)-C(11)	1.554(2)
O(5)-C(16)	1.462(2)	C(10)-H(10A)	0.9900
N(1)-C(5)	1.339(2)	C(10)-H(10B)	0.9900
N(1)-C(6)	1.455(2)	C(11)-C(12)	1.520(2)
N(1)-H(1)	0.880(2)	C(11)-H(11)	1.0000
N(2)-C(12)	1.344(2)	C(13)-C(14)	1.526(2)
N(2)-C(13)	1.461(2)	C(13)-C(15)	1.533(2)
N(2)-H(2)	0.880(2)	C(13)-H(13)	1.0000
C(1)-C(4)	1.526(2)	C(14)-H(14C)	0.9800
C(1)-H(1B)	0.9800	C(14)-H(14A)	0.9800
C(1)-H(1A)	0.9800	C(14)-H(14B)	0.9800
C(1)-H(1C)	0.9800	C(16)-C(17)	1.499(2)
C(2)-C(4)	1.521(2)	C(16)-H(16B)	0.9900
C(2)-H(2A)	0.9800	C(16)-H(16A)	0.9900
C(2)-H(2B)	0.9800	C(17)-C(18)	1.387(3)
C(2)-H(2C)	0.9800	C(17)-C(22)	1.389(2)
C(3)-C(4)	1.524(2)	C(18)-C(19)	1.383(3)
C(3)-H(3B)	0.9800	C(18)-H(18)	0.9500
C(3)-H(3A)	0.9800	C(19)-C(20)	1.379(3)
C(3)-H(3C)	0.9800	C(19)-H(19)	0.9500
C(6)-C(7)	1.529(2)	C(20)-C(21)	1.367(3)
C(6)-H(6B)	0.9900	C(20)-H(20)	0.9500
C(6)-H(6A)	0.9900	C(21)-C(22)	1.400(3)
C(7)-C(8)	1.546(2)	C(21)-H(21)	0.9500
C(7)-C(11)	1.549(2)	C(22)-H(22)	0.9500
C(7)-H(7)	1.0000		
C(8)-C(9)	1.525(3)		
C(5)-O(1)-C(4)	120.52(13)		
C(15)-O(5)-C(16)	115.87(13)		
C(5)-N(1)-C(6)	121.51(13)		
C(5)-N(1)-H(1)	117.6(14)		
C(6)-N(1)-H(1)	118.6(14)		
C(12)-N(2)-C(13)	120.03(13)		
C(12)-N(2)-H(2)	121.7(12)		
C(13)-N(2)-H(2)	117.6(12)		
C(4)-C(1)-H(1B)	109.5		
C(4)-C(1)-H(1A)	109.5		
H(1B)-C(1)-H(1A)	109.5		
C(4)-C(1)-H(1C)	109.5		
H(1B)-C(1)-H(1C)	109.5		
H(1A)-C(1)-H(1C)	109.5		
C(4)-C(2)-H(2A)	109.5		
C(4)-C(2)-H(2B)	109.5		
H(2A)-C(2)-H(2B)	109.5		
C(4)-C(2)-H(2C)	109.5		
H(2A)-C(2)-H(2C)	109.5		
H(2B)-C(2)-H(2C)	109.5		
C(4)-C(3)-H(3B)	109.5		
C(4)-C(3)-H(3A)	109.5		

H(3B)-C(3)-H(3A)	109.5	C(14)-C(13)-H(13)	107.5
C(4)-C(3)-H(3C)	109.5	C(15)-C(13)-H(13)	107.5
H(3B)-C(3)-H(3C)	109.5	C(13)-C(14)-H(14C)	109.5
H(3A)-C(3)-H(3C)	109.5	C(13)-C(14)-H(14A)	109.5
O(1)-C(4)-C(2)	102.38(14)	H(14C)-C(14)-H(14A)	109.5
O(1)-C(4)-C(3)	109.72(13)	C(13)-C(14)-H(14B)	109.5
C(2)-C(4)-C(3)	110.42(15)	H(14C)-C(14)-H(14B)	109.5
O(1)-C(4)-C(1)	110.21(13)	H(14A)-C(14)-H(14B)	109.5
C(2)-C(4)-C(1)	109.89(15)	O(4)-C(15)-O(5)	124.55(14)
C(3)-C(4)-C(1)	113.64(15)	O(4)-C(15)-C(13)	124.62(14)
O(2)-C(5)-N(1)	124.26(14)	O(5)-C(15)-C(13)	110.76(13)
O(2)-C(5)-O(1)	125.56(15)	O(5)-C(16)-C(17)	105.96(14)
N(1)-C(5)-O(1)	110.16(13)	O(5)-C(16)-H(16B)	110.5
N(1)-C(6)-C(7)	112.44(11)	C(17)-C(16)-H(16B)	110.5
N(1)-C(6)-H(6B)	109.1	O(5)-C(16)-H(16A)	110.5
C(7)-C(6)-H(6B)	109.1	C(17)-C(16)-H(16A)	110.5
N(1)-C(6)-H(6A)	109.1	H(16B)-C(16)-H(16A)	108.7
C(7)-C(6)-H(6A)	109.1	C(18)-C(17)-C(22)	118.49(16)
H(6B)-C(6)-H(6A)	107.8	C(18)-C(17)-C(16)	120.77(15)
C(6)-C(7)-C(8)	111.68(12)	C(22)-C(17)-C(16)	120.70(17)
C(6)-C(7)-C(11)	111.48(12)	C(19)-C(18)-C(17)	120.91(16)
C(8)-C(7)-C(11)	105.28(13)	C(19)-C(18)-H(18)	119.5
C(6)-C(7)-H(7)	109.4	C(17)-C(18)-H(18)	119.5
C(8)-C(7)-H(7)	109.4	C(20)-C(19)-C(18)	120.07(19)
C(11)-C(7)-H(7)	109.4	C(20)-C(19)-H(19)	120.0
C(9)-C(8)-C(7)	104.68(13)	C(18)-C(19)-H(19)	120.0
C(9)-C(8)-H(8B)	110.8	C(21)-C(20)-C(19)	120.10(18)
C(7)-C(8)-H(8B)	110.8	C(21)-C(20)-H(20)	120.0
C(9)-C(8)-H(8A)	110.8	C(19)-C(20)-H(20)	120.0
C(7)-C(8)-H(8A)	110.8	C(20)-C(21)-C(22)	120.08(17)
H(8B)-C(8)-H(8A)	108.9	C(20)-C(21)-H(21)	120.0
C(8)-C(9)-C(10)	102.70(14)	C(22)-C(21)-H(21)	120.0
C(8)-C(9)-H(9B)	111.2	C(17)-C(22)-C(21)	120.35(19)
C(10)-C(9)-H(9B)	111.2	C(17)-C(22)-H(22)	119.8
C(8)-C(9)-H(9A)	111.2	C(21)-C(22)-H(22)	119.8
C(10)-C(9)-H(9A)	111.2		
H(9B)-C(9)-H(9A)	109.1		
C(9)-C(10)-C(11)	102.93(13)		
C(9)-C(10)-H(10A)	111.2		
C(11)-C(10)-H(10A)	111.2		
C(9)-C(10)-H(10B)	111.2		
C(11)-C(10)-H(10B)	111.2		
H(10A)-C(10)-H(10B)	109.1		
C(12)-C(11)-C(7)	114.05(13)		
C(12)-C(11)-C(10)	110.54(12)		
C(7)-C(11)-C(10)	105.85(12)		
C(12)-C(11)-H(11)	108.8		
C(7)-C(11)-H(11)	108.8		
C(10)-C(11)-H(11)	108.8		
O(3)-C(12)-N(2)	121.81(14)		
O(3)-C(12)-C(11)	123.41(13)		
N(2)-C(12)-C(11)	114.71(14)		
N(2)-C(13)-C(14)	112.43(13)		
N(2)-C(13)-C(15)	110.49(12)		
C(14)-C(13)-C(15)	111.19(14)		
N(2)-C(13)-H(13)	107.5		



Table 4. Anisotropic displacement parameters ( $\text{\AA}^2 \times 10^3$ ) for gellman142. The anisotropic displacement factor exponent takes the form:  $-2\pi^2 [ h^2 a^{*2} U^{11} + \dots + 2 h k a^* b^* U^{12} ]$

	U <sup>11</sup>	U <sup>22</sup>	U <sup>33</sup>	U <sup>23</sup>	U <sup>13</sup>	U <sup>12</sup>
O(1)	17(1)	25(1)	31(1)	8(1)	5(1)	4(1)
O(2)	16(1)	27(1)	28(1)	0(1)	2(1)	3(1)
O(3)	16(1)	25(1)	25(1)	-2(1)	4(1)	7(1)
O(4)	31(1)	26(1)	26(1)	-2(1)	7(1)	9(1)
O(5)	27(1)	25(1)	21(1)	6(1)	7(1)	8(1)
N(1)	14(1)	24(1)	19(1)	2(1)	3(1)	3(1)
N(2)	15(1)	21(1)	21(1)	3(1)	4(1)	5(1)
C(1)	27(1)	27(1)	26(1)	-1(1)	2(1)	6(1)
C(2)	30(1)	28(1)	61(1)	16(1)	16(1)	11(1)
C(3)	34(1)	47(1)	24(1)	8(1)	6(1)	21(1)
C(4)	21(1)	28(1)	29(1)	7(1)	6(1)	10(1)
C(5)	17(1)	25(1)	14(1)	1(1)	0(1)	2(1)
C(6)	20(1)	20(1)	23(1)	-3(1)	2(1)	4(1)
C(7)	16(1)	17(1)	25(1)	2(1)	6(1)	3(1)
C(8)	23(1)	19(1)	37(1)	5(1)	8(1)	3(1)
C(9)	29(1)	21(1)	36(1)	7(1)	8(1)	9(1)
C(10)	25(1)	25(1)	24(1)	7(1)	6(1)	10(1)
C(11)	17(1)	20(1)	18(1)	3(1)	5(1)	6(1)
C(12)	20(1)	20(1)	16(1)	6(1)	3(1)	6(1)
C(13)	20(1)	20(1)	22(1)	0(1)	0(1)	2(1)
C(14)	32(1)	21(1)	26(1)	3(1)	3(1)	5(1)
C(15)	23(1)	21(1)	18(1)	-1(1)	-1(1)	4(1)
C(16)	35(1)	32(1)	24(1)	8(1)	15(1)	8(1)
C(17)	31(1)	29(1)	18(1)	4(1)	11(1)	3(1)
C(18)	35(1)	28(1)	24(1)	0(1)	4(1)	3(1)
C(19)	48(1)	33(1)	32(1)	5(1)	10(1)	14(1)
C(20)	69(2)	24(1)	33(1)	2(1)	23(1)	5(1)
C(21)	61(1)	35(1)	31(1)	-7(1)	12(1)	-18(1)
C(22)	38(1)	44(1)	26(1)	3(1)	3(1)	-6(1)

Table 5. Hydrogen coordinates ( $\times 10^4$ ) and isotropic displacement parameters ( $\text{\AA}^2 \times 10^{-3}$ ) for gellman142.

	x	y	z	U(eq)
H(1)	36(13)	1057(19)	4357(19)	28(5)
H(2)	-3559(17)	301(18)	737(17)	24(5)
H(1B)	6934	-1018	3520	40
H(1A)	4139	-1842	2817	40
H(1C)	6205	-2616	3550	40
H(2A)	684	-3094	4032	57
H(2B)	850	-2771	5485	57
H(2C)	2788	-3674	4945	57
H(3B)	4993	-1218	6577	49
H(3A)	7386	-564	5800	49
H(3C)	6890	-2132	6016	49
H(6B)	4166	3281	4495	26
H(6A)	994	3312	4287	26
H(7)	4184	2550	2429	23
H(8B)	3565	5025	3004	31
H(8A)	4162	4559	1649	31
H(9B)	71	5265	1239	33
H(9A)	-1104	4625	2447	33
H(10A)	-252	3151	246	28
H(10B)	-3039	2980	886	28
H(11)	-1436	1856	2470	21
H(13)	-3708	-1258	-713	25
H(14C)	-2545	-2537	902	40
H(14A)	622	-1955	844	40
H(14B)	-1110	-2909	-273	40
H(16B)	1585	911	-3134	35
H(16A)	3776	1321	-1943	35
H(18)	-1736	2449	-3613	35
H(19)	-2380	4649	-3618	44
H(20)	533	6325	-2352	50
H(21)	4108	5811	-1097	55
H(22)	4805	3598	-1096	46

Table 6. Torsion angles [ $^{\circ}$ ] for gellman142.

---

C(5)-O(1)-C(4)-C(2)	-177.67(13)
C(5)-O(1)-C(4)-C(3)	65.06(17)
C(5)-O(1)-C(4)-C(1)	-60.80(17)
C(6)-N(1)-C(5)-O(2)	10.9(2)
C(6)-N(1)-C(5)-O(1)	-170.49(11)
C(4)-O(1)-C(5)-O(2)	0.2(2)
C(4)-O(1)-C(5)-N(1)	-178.36(11)
C(5)-N(1)-C(6)-C(7)	74.93(17)
N(1)-C(6)-C(7)-C(8)	172.11(13)
N(1)-C(6)-C(7)-C(11)	54.65(17)
C(6)-C(7)-C(8)-C(9)	-99.05(15)
C(11)-C(7)-C(8)-C(9)	22.08(16)
C(7)-C(8)-C(9)-C(10)	-40.22(16)
C(8)-C(9)-C(10)-C(11)	42.26(15)
C(6)-C(7)-C(11)-C(12)	-112.94(14)
C(8)-C(7)-C(11)-C(12)	125.79(13)
C(6)-C(7)-C(11)-C(10)	125.32(13)
C(8)-C(7)-C(11)-C(10)	4.05(15)
C(9)-C(10)-C(11)-C(12)	-152.51(13)
C(9)-C(10)-C(11)-C(7)	-28.54(16)
C(13)-N(2)-C(12)-O(3)	-6.25(19)
C(13)-N(2)-C(12)-C(11)	170.63(12)
C(7)-C(11)-C(12)-O(3)	-13.25(19)
C(10)-C(11)-C(12)-O(3)	105.87(16)
C(7)-C(11)-C(12)-N(2)	169.92(11)
C(10)-C(11)-C(12)-N(2)	-70.96(16)
C(12)-N(2)-C(13)-C(14)	79.69(16)
C(12)-N(2)-C(13)-C(15)	-45.19(17)
C(16)-O(5)-C(15)-O(4)	-9.8(2)
C(16)-O(5)-C(15)-C(13)	173.03(12)
N(2)-C(13)-C(15)-O(4)	142.28(15)
C(14)-C(13)-C(15)-O(4)	16.7(2)
N(2)-C(13)-C(15)-O(5)	-40.53(16)
C(14)-C(13)-C(15)-O(5)	-166.11(12)
C(15)-O(5)-C(16)-C(17)	-169.85(12)
O(5)-C(16)-C(17)-C(18)	-77.86(18)
O(5)-C(16)-C(17)-C(22)	99.59(18)
C(22)-C(17)-C(18)-C(19)	-0.5(2)
C(16)-C(17)-C(18)-C(19)	176.97(16)
C(17)-C(18)-C(19)-C(20)	-0.1(3)
C(18)-C(19)-C(20)-C(21)	0.4(3)
C(19)-C(20)-C(21)-C(22)	-0.1(3)
C(18)-C(17)-C(22)-C(21)	0.8(2)
C(16)-C(17)-C(22)-C(21)	-176.67(16)
C(20)-C(21)-C(22)-C(17)	-0.5(3)

---

Symmetry transformations used to generate equivalent atoms:

Table 7. Hydrogen bonds for gellman142 [ $\text{\AA}$  and  $^\circ$ ].

D-H...A	d(D-H)	d(H...A)	d(D...A)	$\angle(\text{DHA})$
N(1)-H(1)...O(2)#1	0.880(2)	2.024(10)	2.835(2)	152.8(19)
N(2)-H(2)...O(3)#1	0.880(2)	2.084(3)	2.964(2)	178.7(18)

Symmetry transformations used to generate equivalent atoms:

#1  $x-1, y, z$